

# *Equation of motion and vorticity transport*

---

- 6.1 Newton's second law of motion for a fluid parcel**
- 6.2 Integral momentum balance**
- 6.3 Cauchy's equation of motion**
- 6.4 Euler and Bernoulli equations**
- 6.5 The Navier–Stokes equation**
- 6.6 Vorticity transport**
- 6.7 Dynamic similitude and the Reynolds number**
- 6.8 Structure of a flow as a function of the Reynolds number**
- 6.9 Dimensionless numbers in fluid dynamics**

Fluid flow is established in response to an external action mediated by boundary motion, by the application of a surface force, or by the presence of a body force. The evolution of a transient flow and the structure of a steady flow established after an initial start-up period of time are governed by two fundamental principles of thermodynamics and classical mechanics: mass conservation, and Newton's second law for the motion of a fluid parcel. The implementation of Newton's law of motion in continuum mechanics leads us to Cauchy's equation of motion, which provides us with an expression for the point particle acceleration in terms of stresses, and to the vorticity transport equation governing the point particle rotation. The derivation and interpretation of these governing equations in general and specific terms, and their solution for simple flow configurations are discussed in this chapter.

## **6.1 Newton's second law of motion for a fluid parcel**

Consider a fluid parcel in motion, as illustrated in [Figure 6.1.1](#). Newton's second law of motion requires that the rate of change of the parcel's linear momentum,  $\mathbf{M}_{\text{parcel}}$ , must be equal to the sum of the forces exerted on the parcel at any instant. The forces include the surface force given in equation (5.1.2) and the body force due to gravity given in equation (5.1.1),

$$\frac{d\mathbf{M}_{\text{parcel}}}{dt} = \mathbf{F}^{\text{surface}} + \mathbf{F}^{\text{body}}. \quad (6.1.1)$$

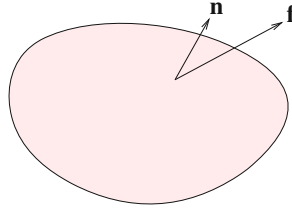


**Figure 6.1.1** Illustration of a fluid parcel in motion, showing the unit normal vector,  $\mathbf{n}$ , and the traction vector,  $\mathbf{f}$ . The motion of the parcel is governed by Newton's second law of motion.

Expressing the surface force in terms of the traction exerted on the parcel surface,  $\mathbf{f}$ , and the body force in terms of the fluid density,  $\rho$ , and the acceleration of gravity,  $\mathbf{g}$ , we obtain

$$\frac{d\mathbf{M}_{\text{parcel}}}{dt} = \iiint_{\text{parcel}} \mathbf{f} dS + \iiint_{\text{parcel}} \rho \mathbf{g} dV. \quad (6.1.2)$$

Expressing the traction in terms of the stress tensor, as shown in (4.2.10), we obtain

$$\frac{d\mathbf{M}_{\text{parcel}}}{dt} = \iiint_{\text{parcel}} \mathbf{n} \cdot \boldsymbol{\sigma} dS + \iiint_{\text{parcel}} \rho \mathbf{g} dV, \quad (6.1.3)$$

where the unit normal vector,  $\mathbf{n}$ , points into the parcel exterior. Our next task is to relate the rate of change of the parcel momentum to the fluid density and velocity.

### 6.1.1 Rate of change of linear momentum

An expression for the linear momentum arises by subdividing a parcel into elementary subparcels with volume  $dV_{\text{parcel}}$  and corresponding mass  $dm_{\text{parcel}} = \rho dV_{\text{parcel}}$ , and summing the contributions by integration to obtain

$$\mathbf{M}_{\text{parcel}} = \iiint_{\text{parcel}} \mathbf{u} dm = \iiint_{\text{parcel}} \mathbf{u} \rho dV, \quad (6.1.4)$$

where  $\mathbf{u}$  is the fluid velocity. The rate of change of the parcel's linear momentum is given by

$$\frac{d\mathbf{M}_{\text{parcel}}}{dt} = \frac{d}{dt} \iiint_{\text{parcel}} \mathbf{u} dm = \frac{d}{dt} \iiint_{\text{parcel}} \mathbf{u} \rho dV, \quad (6.1.5)$$

where the time derivative is taken for a fixed parcel identity.

Because the integral is computed over the volume of the parcel, which is not stationary but changes in time, switching the order of time differentiation and volume integration on the right-hand side of (6.1.5) is permissible only if the time derivative is replaced by the material derivative,  $D/Dt$ , under the integral sign, yielding

$$\frac{d\mathbf{M}_{\text{parcel}}}{dt} = \iiint_{\text{parcel}} \frac{D(\mathbf{u} dm)}{Dt} = \iiint_{\text{parcel}} \left( \frac{D\mathbf{u}}{Dt} dm + \frac{D dm}{Dt} \mathbf{u} \right). \quad (6.1.6)$$

Mass conservation requires that the material derivative of the elementary mass,  $dm$  should be zero, yielding the simplified expression

$$\frac{dM_{\text{parcel}}}{dt} = \iiint_{\text{parcel}} \frac{D\mathbf{u}}{Dt} dm = \iiint_{\text{parcel}} \frac{D\mathbf{u}}{Dt} \rho dV, \quad (6.1.7)$$

where  $D\mathbf{u}/Dt$  is the point particle acceleration. The density may vary over the parcel volume.

### 6.1.2 Equation of parcel motion

Substituting the right-hand side of (6.1.7) into the left-hand side of (6.1.3), we obtain the desired equation of parcel motion,

$$\iiint_{\text{parcel}} \frac{D\mathbf{u}}{Dt} \rho dV = \iint_{\text{parcel}} \mathbf{n} \cdot \boldsymbol{\sigma} dS + \iiint_{\text{parcel}} \rho \mathbf{g} dV, \quad (6.1.8)$$

involving the point particle acceleration, the stress tensor, and the body force. Explicitly, the  $x$ ,  $y$ , and  $z$  components of (6.1.8) are

$$\begin{aligned} \iiint_{\text{parcel}} \frac{Du_x}{Dt} \rho dV &= \iint_{\text{parcel}} (n_x \sigma_{xx} + n_y \sigma_{yx} + n_z \sigma_{zx}) dS + \iiint_{\text{parcel}} \rho g_x dV, \\ \iiint_{\text{parcel}} \frac{Du_y}{Dt} \rho dV &= \iint_{\text{parcel}} (n_x \sigma_{xy} + n_y \sigma_{yy} + n_z \sigma_{zy}) dS + \iiint_{\text{parcel}} \rho g_y dV, \\ \iiint_{\text{parcel}} \frac{Du_z}{Dt} \rho dV &= \iint_{\text{parcel}} (n_x \sigma_{xz} + n_y \sigma_{yz} + n_z \sigma_{zz}) dS + \iiint_{\text{parcel}} \rho g_z dV. \end{aligned} \quad (6.1.9)$$

Equations (6.1.10) are valid irrespective of whether the fluid is compressible or incompressible.

### 6.1.3 Two-dimensional flow

The counterpart of the parcel equation of motion (6.1.8) for two-dimensional flow in the  $xy$  plane is

$$\iint_{\text{parcel}} \frac{D\mathbf{u}}{Dt} \rho dA = \oint_{\text{parcel}} \mathbf{n} \cdot \boldsymbol{\sigma} d\ell + \iint_{\text{parcel}} \rho \mathbf{g} dA, \quad (6.1.10)$$

where  $dA$  is a differential area and  $d\ell$  is the differential arc length along the boundary of a parcel in the  $xy$  plane. Explicitly, the  $x$  and  $y$  components of (6.1.10) are

$$\begin{aligned} \iint_{\text{parcel}} \frac{Du_x}{Dt} \rho dA &= \oint_{\text{parcel}} (n_x \sigma_{xx} + n_y \sigma_{yx}) d\ell + \iint_{\text{parcel}} \rho g_x dA, \\ \iint_{\text{parcel}} \frac{Du_y}{Dt} \rho dA &= \oint_{\text{parcel}} (n_x \sigma_{xy} + n_y \sigma_{yy}) d\ell + \iint_{\text{parcel}} \rho g_y dA. \end{aligned} \quad (6.1.11)$$

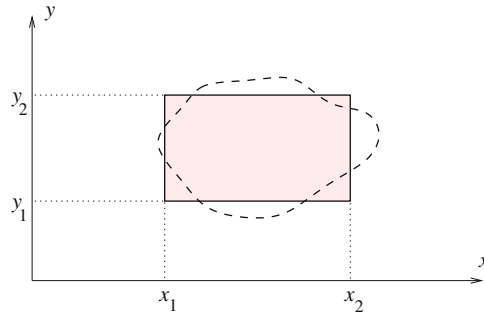


**Figure 6.1.2** Illustration of a fluid parcel with a rectangular instantaneous shape, drawn with the solid line, in a two-dimensional flow. Even though the parcel generally deforms to obtain a warped shape, drawn with the dashed line, Newton's second law of motion in its integral form can be applied over the instantaneous parcel shape.

These equations are valid irrespective of whether the fluid is compressible or incompressible.

### A rectangular parcel

As an application, we consider the motion of a fluid parcel with an instantaneous rectangular shape whose sides are parallel to the  $x$  or  $y$  axis, as depicted in Figure 6.1.2. The parcel will remain rectangular only if the fluid exhibits rigid-body motion. Under more general conditions, the parcel will deform to obtain the warped shape, drawn with the dashed line in Figure 6.1.1. However, parcel deformation does not prevent us from evaluating the integrals in (6.1.11) over the instantaneous rectangular shape.

For simplicity, we assume that the density of the fluid is uniform and the acceleration of gravity is constant over the parcel volume. We note that the unit normal vector is parallel to the  $x$  or  $y$  axis over each side, and find that equations (6.1.11) take the simpler forms

$$\begin{aligned} \int_{x_1}^{x_2} \int_{y_1}^{y_2} \left( \frac{Du_x}{Dt} - g_x \right) \rho \, dy \, dx & \quad (6.1.12) \\ &= \int_{y_1}^{y_2} [(\sigma_{xx})_{x=x_2} - (\sigma_{xx})_{x=x_1}] \, dy + \int_{x_1}^{x_2} [(\sigma_{yx})_{y=y_2} - (\sigma_{yx})_{y=y_1}] \, dx \end{aligned}$$

and

$$\begin{aligned} \int_{x_1}^{x_2} \int_{y_1}^{y_2} \left( \frac{Du_y}{Dt} - g_y \right) \rho \, dy \, dx & \quad (6.1.13) \\ &= \int_{y_1}^{y_2} [(\sigma_{xy})_{x=x_2} - (\sigma_{xy})_{x=x_1}] \, dy + \int_{x_1}^{x_2} [(\sigma_{yy})_{y=y_2} - (\sigma_{yy})_{y=y_1}] \, dx. \end{aligned}$$

The first integral on the right-hand side of (6.1.12) involves normal stresses exerted on the vertical sides; the second integral involves shear stresses exerted on the horizontal sides; the converse is true for (6.1.13).

*Steady unidirectional flow*

In the case of steady unidirectional flow along the  $x$  axis, point particles move along the  $x$  axis with constant velocity and vanishing acceleration,  $D\mathbf{u}/Dt = 0$ . Setting the left-hand side of the equation of parcel motion (6.1.10) to zero, we obtain a balance between the hydrodynamic and the body force,

$$\oint_{\text{parcel}} \mathbf{n} \cdot \boldsymbol{\sigma} \, d\ell + \iint_{\text{parcel}} \rho \mathbf{g} \, dA = \mathbf{0}. \quad (6.1.14)$$

Now restricting our attention to Newtonian fluids, we use the constitutive equation shown in Table 4.5.1 and make two key observations:

- In the absence of axial and transverse stretching,  $\partial u_x/\partial x = 0$  and  $\partial u_y/\partial y = 0$ , the normal stresses  $\sigma_{xx}$  and  $\sigma_{yy}$  are equal to the negative of the pressure,  $\sigma_{xx} = \sigma_{yy} = -p$ .
- The shear stresses  $\sigma_{xy} = \sigma_{yx}$  are independent of streamwise position,  $x$ , but may depend on the lateral position,  $y$ .

Subject to these simplifications, the balance equations (6.1.12) and (6.1.13) reduce to

$$\int_{y_1}^{y_2} (p_{x=x_2} - p_{x=x_1}) \, dy - [(\sigma_{yx})_{y=y_2} - (\sigma_{yx})_{y=y_1}] \Delta x = \rho g_x \Delta x \Delta y \quad (6.1.15)$$

and

$$\int_{x_1}^{x_2} (p_{y=y_2} - p_{y=y_1}) \, dx = \rho g_y \Delta x \Delta y, \quad (6.1.16)$$

where  $\Delta x \equiv x_2 - x_1$  and  $\Delta y = y_2 - y_1$ .

Equation (6.1.16) is satisfied when

$$\frac{p_{x,y=y_2} - p_{x,y=y_1}}{\Delta y} = \rho g_y \quad (6.1.17)$$

for any  $x$ , reflecting the hydrostatic pressure variation. Equation (6.1.15) is satisfied when

$$\frac{p_{x=x_2,y} - p_{x=x_1,y}}{\Delta x} = \rho g_x - \chi \quad (6.1.18)$$

and

$$\frac{(\sigma_{yx})_{x,y=y_2} - (\sigma_{yx})_{x,y=y_1}}{\Delta y} = -\chi, \quad (6.1.19)$$

where  $\chi$  is a free parameter. Physically, the constant  $\chi$  is determined by the mechanism driving the flow. Three modular flow configurations can be identified, as discussed next.

*Shear-driven flow*

When  $\chi = 0$ , equation (6.1.18) shows that the pressure variation in the direction of the  $x$  axis is hydrostatic. Equation (6.1.19) shows that the shear stress  $\sigma_{yx}$  is constant, independent of  $y$ ,

$$(\sigma_{yx})_{x,y=y_2} - (\sigma_{yx})_{x,y=y_1} = 0. \quad (6.1.20)$$

This is the case of shear-driven flow.

*Gravity-driven flow*

When the streamwise pressure drop is zero,  $p_{x=x_2,y} = p_{x=x_1,y}$ , equation (6.1.18) requires that  $\chi = \rho g_x$ . Equation (6.1.19) shows that the difference in the shear stress is given by

$$(\sigma_{yx})_{x,y=y_2} - (\sigma_{yx})_{x,y=y_1} = -\rho g_x \Delta y. \quad (6.1.21)$$

This is the case of gravity-driven flow.

*Pressure-driven flow*

When the flow is horizontal,  $g_x = 0$ , equation (6.1.18) shows that  $\chi$  is the negative of the streamwise pressure gradient. Equation (6.1.19) shows that the difference in the shear stress is given by

$$(\sigma_{yx})_{x,y=y_2} - (\sigma_{yx})_{x,y=y_1} = -\chi \Delta y. \quad (6.1.22)$$

This is the case of pressure-driven flow.

**PROBLEM****6.1.1** *Body force in terms of a surface integral*

Show that the body force expressed by the second integral on the right-hand side of (6.1.8) can be expressed as a surface integral in the form

$$\iint_{\text{parcel}} \rho (\mathbf{g} \cdot \mathbf{x}) \mathbf{n} \, dS. \quad (6.1.23)$$

*Hint:* Use the Gauss divergence theorem (2.6.36).

**6.2 Integral momentum balance**

Consider the integrand of the rate of change of momentum on the left-hand side of equation (6.1.8). Using the rules of product differentiation and the continuity equation (2.8.5), we write

$$\rho \frac{D\mathbf{u}}{Dt} = \frac{D(\rho\mathbf{u})}{Dt} - \mathbf{u} \frac{D\rho}{Dt} = \frac{D(\rho\mathbf{u})}{Dt} + (\rho\mathbf{u})(\nabla \cdot \mathbf{u}), \quad (6.2.1)$$

where

$$\nabla \cdot \mathbf{u} \equiv \frac{\partial u_x}{\partial x} + \frac{\partial u_y}{\partial y} + \frac{\partial u_z}{\partial z} \quad (6.2.2)$$

is the divergence of the velocity expressing the rate of the expansion of the fluid. If the fluid is incompressible, the second term on the right-hand side of (6.2.1) does not appear.

The  $x$  component of the vectorial expression (6.2.1) can be manipulated to give

$$\rho \frac{Du_x}{Dt} = \frac{D(\rho u_x)}{Dt} + (\rho u_x) (\nabla \cdot \mathbf{u}) \quad (6.2.3)$$

or

$$\rho \frac{Du_x}{Dt} = \frac{\partial(\rho u_x)}{\partial t} + \mathbf{u} \cdot \nabla(\rho u_x) + (\rho u_x) (\nabla \cdot \mathbf{u}), \quad (6.2.4)$$

where the time derivative  $\partial/\partial t$  is taken keeping the spatial position fixed. More explicitly,

$$\rho \frac{Du_x}{Dt} = \frac{\partial(\rho u_x)}{\partial t} + u_x \frac{\partial(\rho u_x)}{\partial x} + u_y \frac{\partial(\rho u_x)}{\partial y} + u_z \frac{\partial(\rho u_x)}{\partial z} + (\rho u_x) (\nabla \cdot \mathbf{u}). \quad (6.2.5)$$

Combining the last four terms in the last expression, we find that

$$\rho \frac{Du_x}{Dt} = \frac{\partial(\rho u_x)}{\partial t} + \frac{\partial(\rho u_x u_x)}{\partial x} + \frac{\partial(\rho u_y u_x)}{\partial y} + \frac{\partial(\rho u_z u_x)}{\partial z}. \quad (6.2.6)$$

This expression applies to incompressible as well as compressible fluids.

Working in a similar fashion with the  $y$  and  $z$  components of (6.2.1), we derive the corresponding expressions

$$\rho \frac{Du_y}{Dt} = \frac{\partial(\rho u_y)}{\partial t} + \frac{\partial(\rho u_x u_y)}{\partial x} + \frac{\partial(\rho u_y u_y)}{\partial y} + \frac{\partial(\rho u_z u_y)}{\partial z} \quad (6.2.7)$$

and

$$\rho \frac{Du_z}{Dt} = \frac{\partial(\rho u_z)}{\partial t} + \frac{\partial(\rho u_x u_z)}{\partial x} + \frac{\partial(\rho u_y u_z)}{\partial y} + \frac{\partial(\rho u_z u_z)}{\partial z}. \quad (6.2.8)$$

These expressions hold true for incompressible as well as compressible fluids.

### Momentum tensor

To recast equations (6.2.6)–(6.2.8) into a unified form, we introduce the momentum tensor,  $M_{ij}$ , defined as

$$M_{ij} \equiv \rho u_i u_j, \quad (6.2.9)$$

where the indices  $i$  and  $j$  range over  $x$ ,  $y$ , and  $z$  or, correspondingly, 1, 2, and 3. In vector notation, we write

$$\mathbf{M} = \rho \mathbf{u} \otimes \mathbf{u}, \quad (6.2.10)$$

where the symbol  $\otimes$  denotes the tensor product. It is evident from the definition (6.2.9) that the tensor  $\mathbf{M}$  is symmetric,

$$M_{ij} = M_{ji}. \quad (6.2.11)$$

Explicitly, the momentum tensor is given by

$$\mathbf{M} = \rho \begin{bmatrix} u_x^2 & u_x u_y & u_x u_z \\ u_y u_x & u_y^2 & u_y u_z \\ u_z u_x & u_z u_y & u_z^2 \end{bmatrix}. \quad (6.2.12)$$

Next, we introduce the divergence of the momentum tensor defined as a vector whose  $i$ th component is given by

$$(\nabla \cdot \mathbf{M})_i = \frac{\partial M_{ji}}{\partial x_j} = \frac{\partial M_{ij}}{\partial x_j}, \quad (6.2.13)$$

where summation is implied over the repeated index  $j$ . For example, the  $x$  component of the divergence of  $\mathbf{M}$  is

$$(\nabla \cdot \mathbf{M})_x = \frac{\partial M_{jx}}{\partial x_j} = \frac{\partial M_{xx}}{\partial x} + \frac{\partial M_{yx}}{\partial y} + \frac{\partial M_{zx}}{\partial z}. \quad (6.2.14)$$

Subject to these definitions, equations (6.2.6)–(6.2.8) can be compiled into the form

$$\rho \frac{Du_i}{Dt} = \frac{\partial(\rho u_i)}{\partial t} + \frac{\partial M_{ji}}{\partial x_j} \quad (6.2.15)$$

for  $i = x, y, z$ . The corresponding vector form is

$$\rho \frac{D\mathbf{u}}{Dt} = \frac{\partial(\rho \mathbf{u})}{\partial t} + \nabla \cdot \mathbf{M}. \quad (6.2.16)$$

The right-hand sides of equations (6.2.15) and (6.2.16) involve Eulerian derivatives; that is, derivatives with respect to time and spatial coordinates.

### Equation of parcel motion

Substituting (6.2.16) into the left-hand side of the equation of parcel motion (6.1.8), we derive the alternative form

$$\iiint_{\text{parcel}} \left( \frac{\partial(\rho \mathbf{u})}{\partial t} + \nabla \cdot \mathbf{M} \right) dV = \iint_{\text{parcel}} \mathbf{n} \cdot \boldsymbol{\sigma} dS + \iiint_{\text{parcel}} \rho \mathbf{g} dV. \quad (6.2.17)$$

We can use the Gauss divergence theorem stated in equation (2.6.36) to convert the volume integral of the divergence of the momentum tensor into a surface integral over the parcel volume, obtaining

$$\iiint_{\text{parcel}} \frac{\partial(\rho \mathbf{u})}{\partial t} dV + \iint_{\text{parcel}} \mathbf{n} \cdot \mathbf{M} dS = \iint_{\text{parcel}} \mathbf{n} \cdot \boldsymbol{\sigma} dS + \iiint_{\text{parcel}} \rho \mathbf{g} dV, \quad (6.2.18)$$



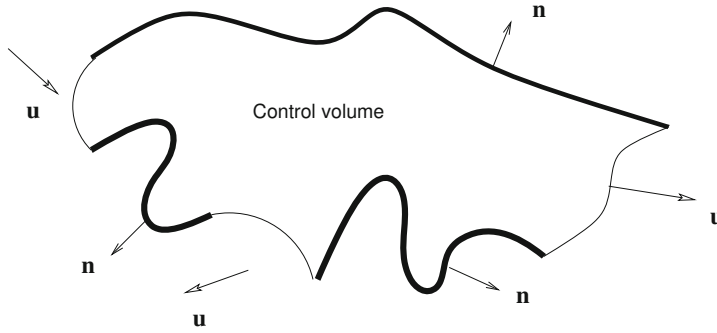


**Figure 6.2.1** Illustration of a stationary control volume (cv) in a flow bounded by solid or fluid surfaces.

where the unit normal vector,  $\mathbf{n}$ , points outward from the parcel. In index notation,

$$\iiint_{\text{parcel}} \frac{\partial(\rho u_i)}{\partial t} dV + \iint_{\text{parcel}} n_j M_{ji} dS = \iint_{\text{parcel}} n_j \sigma_{ji} dS + \iiint_{\text{parcel}} \rho g_i dV \quad (6.2.19)$$

for  $i = x, y, z$ , where summation is implied over the repeated index  $j$ .

### 6.2.1 Control volume and integral momentum balance

It is important to bear in mind that equation (6.2.19) originates from Newton's second law of motion applied to a fluid parcel. In the process of expressing the material derivative in terms of Eulerian derivatives taken with respect to time and position in space, the parcel has lost its significance as a material body and became relevant only insofar as to define the volume it occupies in space at any instant.

To emphasize the new interpretation, we rewrite the integral momentum balance (6.2.19) in identical form, except that the volume of integration is now regarded as a control volume (cv), as shown in [Figure 6.2.1](#).

Using the definition of the momentum tensor shown in (6.2.9), we express the integral momentum balance in the form

$$\iiint_{\text{cv}} \frac{\partial(\rho u_i)}{\partial t} dV + \iint_{\text{cv}} \rho u_i u_n dS = \iint_{\text{cv}} n_j \sigma_{ji} dS + \iiint_{\text{cv}} \rho g_i dV, \quad (6.2.20)$$

where  $i = x, y, z$  is a free index, summation is implied over the repeated index,  $j$ , and

$$u_n \equiv \mathbf{u} \cdot \mathbf{n} = u_j n_j \quad (6.2.21)$$

is the normal component of the fluid velocity. Equation (6.2.20) expresses an *integral momentum balance*, well known to chemical engineers and others in the framework of transport phenomena.

*Accumulation, convection, boundary and homogeneous forcing*

The four integrals on the left- and right-hand sides of (6.2.20) admit the following interpretation with regard to the underlying control volume:

1. The first integral is the rate of change of the  $i$ th component of momentum of the fluid residing inside the control volume. At steady state, this term vanishes.
2. The scalar  $n_j u_j = \mathbf{n} \cdot \mathbf{u}$  in the second integrand on the left-hand side is the component of the fluid velocity normal to the boundary of the control volume. The corresponding integral expresses the rate of convective transport of the  $i$ th component of the fluid momentum across the boundary of the control volume.
3. The first integral on the right-hand side is the  $i$ th component of the surface force exerted on the boundary of the control volume.
4. The second integral on the right-hand side is the  $i$ th component of the body force exerted on the control volume.

It is important to bear in mind that the integral momentum balance has been derived in Cartesian coordinates. Every term must be rederived when working in polar or other curvilinear coordinates.

*Vector form of the integral momentum balance*

In vector notation, the integral momentum balance takes the form

$$\iiint_{cv} \frac{\partial(\rho \mathbf{u})}{\partial t} dV + \iint_{cv} \rho \mathbf{n} \cdot (\mathbf{u} \otimes \mathbf{u}) dS = \iint_{cv} \mathbf{n} \cdot \boldsymbol{\sigma} dS + \iiint_{cv} \rho \mathbf{g} dV. \quad (6.2.22)$$

The second integral on the left-hand side is given by

$$\iint_{cv} \rho \mathbf{n} \cdot (\mathbf{u} \otimes \mathbf{u}) dS = \iint_{cv} (\rho \mathbf{u}) u_n dS, \quad (6.2.23)$$

where  $u_n = \mathbf{n} \cdot \mathbf{u}$  is the normal velocity and the symbol  $\otimes$  denotes the tensor product.

*Stress-momentum tensor*

Combining the second integral on the left-hand side with the first integral on the right-hand side of (6.2.22), we obtain the more compact form

$$\iiint_{cv} \frac{\partial(\rho \mathbf{u})}{\partial t} dV = \iint_{cv} \mathbf{n} \cdot \boldsymbol{\tau} dS + \iiint_{cv} \rho \mathbf{g} dV, \quad (6.2.24)$$

where

$$\boldsymbol{\tau} \equiv \boldsymbol{\sigma} - \rho \mathbf{u} \otimes \mathbf{u} \quad (6.2.25)$$

is the stress-momentum tensor with components  $\tau_{ij} = \sigma_{ij} - \rho u_i u_j$ .

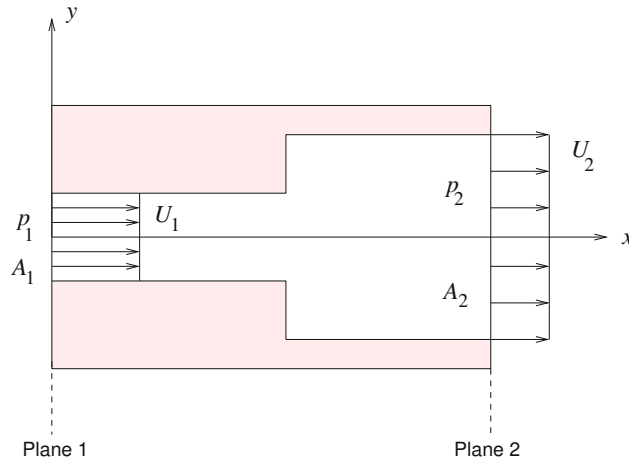


**Figure 6.2.1** Simplified model of flow through a duct with a sudden enlargement. An integral momentum balance allows us to compute the rise in pressure,  $p_2 - p_1$ , in terms of the inlet and outlet cross-sectional areas,  $A_1$  and  $A_2$ .

### *Applications in engineering analysis*

Equation (6.2.24) expresses an integral momentum balance that can be interpreted as an integral evolution equation or conservation law applied to a chosen control volume. The solution of practical engineering problems by the use of integral mass, momentum, and energy balances is discussed in a classical text by Bird, Stewart and Lightfoot.<sup>1</sup> Illustrative examples are presented in the remainder of this section.

### **6.2.2 Flow through a sudden enlargement**

To demonstrate the usefulness of the integral momentum balance in engineering analysis, we consider steady flow through a duct with a sudden enlargement, as illustrated in [Figure 6.2.1](#).

We begin by introducing a control volume identified with the section of the duct confined between the vertical planes labeled 1 and 2, and assume that the density of the fluid is uniform and the velocity profile is flat at the inlet and outlet. The cross-sectional areas at the inlet and outlet are denoted as  $A_1$  and  $A_2$ .

Neglecting the shear stress at the walls, approximating the normal stress at the inlet and outlet with the negative of the pressure, assuming that the pressure at the washer-shaped area is equal to the inlet pressure, and considering the effects of gravity insignificant, we find that the  $x$  component of the integral momentum balance (6.2.20) at steady state simplifies

<sup>1</sup>Bird, R. B., Stewart, W. E. & Lightfoot, E. N. (2006) *Transport Phenomena*, Second Edition, Wiley.

into

$$\rho U_2^2 A_2 - \rho U_1^2 A_1 = -p_2 A_2 + p_1 A_1 + p_1 (A_2 - A_1). \quad (6.2.26)$$

The three terms on the right-hand side of (6.2.26) are approximations to the first integral on the right-hand side of (6.2.20) for the outlet, washer-shaped area, and inlet. Mass conservation requires that

$$U_1 A_1 = U_2 A_2. \quad (6.2.27)$$

Solving for  $U_1$  and substituting the result into (6.2.26), we derive the desired expression for the pressure difference,

$$p_2 - p_1 = (\beta - 1) \rho U_2^2, \quad (6.2.28)$$

where  $\beta = A_2/A_1$  is the area ratio, which predicts a rise in pressure for  $\beta > 1$ , in agreement with laboratory observations.

### 6.2.3 Isentropic flow through a conduit

In a second application, we consider the flow of a compressible fluid through a conduit with variable cross-sectional area,  $A$ . A mass balance over a control volume confined between two cross-sections labeled 1 and 2 requires that

$$\rho_1 U_1 A_1 = \rho_2 U_2 A_2. \quad (6.2.29)$$

The counterpart of equation (6.2.26) is

$$\rho_2 U_2^2 A_2 - \rho_1 U_1^2 A_1 = -p_2 A_2 + p_1 A_1 - D_x, \quad (6.2.30)$$

where  $D_x$  is the drag force due to wall friction. In the case of isentropic flow, we use equation (4.7.23) and find that

$$\frac{p_1}{\rho_1^k} = \frac{p_2}{\rho_2^k} \quad (6.2.31)$$

where  $k \equiv c_p/c_v$  is the ratio of two heat capacities. The last three equations can be used to compute  $p_2$ ,  $U_2$ , and  $D_x$ , from knowledge of  $p_1$ ,  $\rho_1$ , and  $U_1$ .

#### *Energetics*

Energy conservation under adiabatic conditions requires that

$$h_1 + \frac{1}{2} U_1^2 + g y_1 = h_2 + \frac{1}{2} U_2^2 + g y_2, \quad (6.2.32)$$

where  $h$  is the specific enthalpy and  $y$  is the vertical position of the conduit centerline. In terms of the heat capacity under constant pressure,  $h = c_p T$ , yielding

$$c_p T_1 + \frac{1}{2} U_1^2 + g y_1 = c_p T_2 + \frac{1}{2} U_2^2 + g y_2, \quad (6.2.33)$$

where  $T$  is the absolute temperature. This equation relates the velocity to the temperature to the elevation of the conduit centerline at two stations.

### Stagnation-point temperature

At a stagnation point,  $U_2 = 0$ . Equation (6.2.33) with  $y_1 = y_2$  and  $U \equiv U_1$ ,  $T \equiv T_1$ ,  $T_2 \equiv T_{\text{sp}}$  yields

$$T_{\text{sp}} - T = \frac{1}{2} \frac{U_1^2}{c_p} = \frac{1}{2} \frac{k-1}{k} \frac{U^2}{R} \quad (6.2.34)$$

or

$$T_{\text{sp}} - T = \frac{1}{2} (k-1) \frac{U^2}{c^2} T, \quad (6.2.35)$$

where  $c$  is the speed of sound given in (4.7.27). Rearranging, we derive an expression for the stagnation-point temperature,

$$\frac{T_{\text{sp}} - T}{T} = \frac{1}{2} (k-1) M^2, \quad (6.2.36)$$

where

$$M \equiv \frac{U}{c} \quad (6.2.37)$$

is the Mach number. Using the equation of state for isentropic conditions, we obtain

$$\frac{p_2}{p_1} = \left( \frac{1}{2} (k-1) M^2 + 1 \right)^{k/(k-1)}. \quad (6.2.38)$$

For sufficiently small Mach numbers,

$$\frac{p_2}{p_1} \simeq 1 + \frac{1}{2} k M^2, \quad (6.2.39)$$

providing us with a convenient expression for the pressure ratio.

## PROBLEM

### 6.2.1 Pressure rise in an ejector pump

A schematic illustration of an ejector pump is shown in [Figure 6.2.2](#). At plane 1, two fluid streams merge: the first stream with uniform velocity  $U_1$  over a cross-sectional area  $A_1$ , and the second stream with uniform velocity  $U_0$  over a cross sectional area  $A_0$ . At plane 2, the velocity profile is uniform over the cross-sectional area  $A_2 = A_0 + A_1$ . The pressure is assumed to be uniform over the cross-section of the inlet and outlet, respectively, equal to  $p_1$  and  $p_2$ . The fluid density is assumed to be uniform throughout the flow. Derive an expression for the rise in pressure,  $p_2 - p_1$ , in terms of  $\rho$ ,  $U_0$ ,  $U_1$ ,  $A_0$ , and  $A_1$ , similar to that shown in equation (6.2.28).

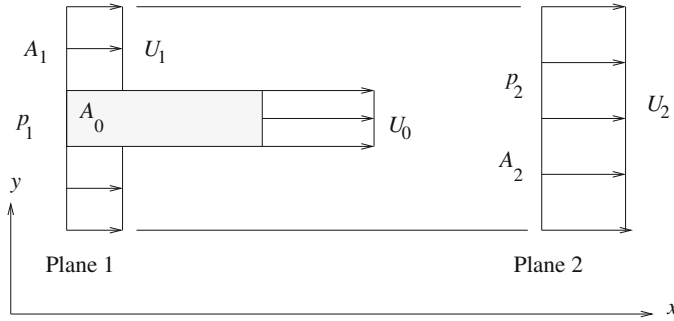


**Figure 6.2.2** Schematic illustration of an ejector pump. The pressure rise between the inlet and outlet,  $p_2 - p_1$ , can be estimated by performing an integral momentum balance.

### 6.3 Cauchy's equation of motion

Equation (6.1.8), repeated below for convenience,

$$\iiint_{\text{parcel}} \frac{D\mathbf{u}}{Dt} \rho \, dV = \iint_{\text{parcel}} \mathbf{n} \cdot \boldsymbol{\sigma} \, dS + \iiint_{\text{parcel}} \rho \mathbf{g} \, dV, \tag{6.3.1}$$

contains one surface integral involving the traction over the boundary of a fluid parcel, and two volume integrals involving the point particle acceleration and the body force.

If we could manage to convert the surface integral into a volume integral, we would be able to collect all integrands into a unified integrand. Since the shape and volume of the parcel is arbitrary, the unified integrand would have to be identically zero, providing us with a differential equation.

#### 6.3.1 Hydrodynamic volume force

Transforming the surface integral of the traction into a volume integral can be done using once again the Gauss divergence theorem stated in equation (2.6.36). Identifying the vector  $\mathbf{h}$  with each one of the three columns of the stress tensor, we obtain

$$\iint_{\text{parcel}} \mathbf{n} \cdot \boldsymbol{\sigma} \, dS = \iiint_{\text{parcel}} \nabla \cdot \boldsymbol{\sigma} \, dV. \tag{6.3.2}$$

In index notation, the  $i$ th component of this equation is

$$\iint_{\text{parcel}} n_j \sigma_{ji} \, dS = \iiint_{\text{parcel}} \frac{\partial \sigma_{ji}}{\partial x_j} \, dV, \tag{6.3.3}$$

where summation of the repeated index  $j$  is implied.

The divergence of the stress tensor under the integral sign on the right-hand side of (6.3.2) is a vector denoted by

$$\boldsymbol{\Sigma} \equiv \nabla \cdot \boldsymbol{\sigma}, \tag{6.3.4}$$

with Cartesian components

$$\begin{aligned}\Sigma_x &= \frac{\partial\sigma_{xx}}{\partial x} + \frac{\partial\sigma_{yx}}{\partial y} + \frac{\partial\sigma_{zx}}{\partial z}, & \Sigma_y &= \frac{\partial\sigma_{xy}}{\partial x} + \frac{\partial\sigma_{yy}}{\partial y} + \frac{\partial\sigma_{zy}}{\partial z}, \\ \Sigma_z &= \frac{\partial\sigma_{xz}}{\partial x} + \frac{\partial\sigma_{yz}}{\partial y} + \frac{\partial\sigma_{zz}}{\partial z}.\end{aligned}\tag{6.3.5}$$

Physically, the vector  $\Sigma$  is the hydrodynamic force per differential volume of fluid; in contrast, the traction  $\mathbf{f}$  is the hydrodynamic force per differential surface area of fluid.

### 6.3.2 Hydrodynamic force on an infinitesimal parcel

To confirm identity (6.3.3), we consider a small fluid parcel in the shape of a rectangular parallelepiped centered at the origin, as illustrated in Figure 5.1.1(b). The six flat sides of the parcel are perpendicular to the  $x$ ,  $y$ , or  $z$  axis, the lengths of the three edges are equal to  $\Delta x$ ,  $\Delta y$ , and  $\Delta z$ , and the volume of the parcel is equal to  $\Delta V = \Delta x \Delta y \Delta z$ .

Consider the surface integral on the left-hand side of equation (6.3.3). Over the sides that are perpendicular to the  $x$  axis, located at  $x = \pm \frac{\Delta x}{2}$ , designated as the *first* or *second* side, the unit normal vector is parallel to the  $x$  axis; over the first side  $n_x = 1$ , and over the second side  $n_x = -1$ . Because the size of the parcel is small, the stresses over each side can be approximated with corresponding values at the center-point.

Subject to this approximation, the surface integral on the left-hand side over the first side takes the form

$$\mathcal{F}_1 \equiv \sigma_{xi}(x = \frac{1}{2} \Delta x, y = 0, z = 0) \Delta y \Delta z,\tag{6.3.6}$$

while the surface integral over the second side takes the form

$$\mathcal{F}_2 \equiv -\sigma_{xi}(x = -\frac{1}{2} \Delta x, y = 0, z = 0) \Delta y \Delta z\tag{6.3.7}$$

for  $i = x, y, z$ , where the parentheses enclose the coordinates of the evaluation point.

Adding these two contributions and factoring out the common product  $\Delta y \Delta z$  expressing the surface area, we obtain

$$\mathcal{F}_1 + \mathcal{F}_2 = \left( \sigma_{xi}(x = \frac{1}{2} \Delta x, y = 0, z = 0) - \sigma_{xi}(x = -\frac{1}{2} \Delta x, y = 0, z = 0) \right) \Delta y \Delta z.\tag{6.3.8}$$

Next, we observe that, in the limit as  $\Delta x$  tends to zero, the ratio of the differences

$$\begin{aligned}& \frac{\sigma_{xi}(x = \frac{\Delta x}{2}, y = 0, z = 0) - \sigma_{xi}(x = -\frac{\Delta x}{2}, y = 0, z = 0)}{\frac{\Delta x}{2} - (-\frac{\Delta x}{2})} \\ &= \frac{\sigma_{xi}(x = \frac{\Delta x}{2}, y = 0, z = 0) - \sigma_{xi}(x = -\frac{\Delta x}{2}, y = 0, z = 0)}{\Delta x}\end{aligned}\tag{6.3.9}$$

tends to the partial derivative  $\partial\sigma_{xi}/\partial x$  evaluated at the origin. Correspondingly, the difference (6.3.8) reduces to

$$\frac{\partial\sigma_{xi}}{\partial x} \Delta x \Delta y \Delta z = \frac{\partial\sigma_{xi}}{\partial x} \Delta V, \quad (6.3.10)$$

where the derivatives are evaluated at the origin.

Working in a similar fashion with pairs of sides that are perpendicular to the  $y$  or  $z$  axis, and summing the three contributions, we find that the left-hand side of (6.3.3) takes the approximate form

$$\left( \frac{\partial\sigma_{xi}}{\partial x} + \frac{\partial\sigma_{yi}}{\partial y} + \frac{\partial\sigma_{zi}}{\partial z} \right) \Delta V, \quad (6.3.11)$$

where the quantity enclosed by the parentheses is evaluated at the origin. Expression (6.3.11) is an approximation to the volume integral on the right-hand side of (6.3.3).

### 6.3.3 The equation of motion

Substituting (6.3.2) into (6.1.8), consolidating various terms, and noting that, since the volume of integration is arbitrary, the combined integrand must vanish, we obtain Cauchy's differential equation governing the motion of an incompressible or compressible fluid,

$$\rho \frac{D\mathbf{u}}{Dt} = \nabla \cdot \boldsymbol{\sigma} + \rho \mathbf{g}. \quad (6.3.12)$$

In index notation,

$$\rho \frac{Du_i}{Dt} = \frac{\partial\sigma_{ji}}{\partial x_j} + \rho g_i, \quad (6.3.13)$$

where summation over the repeated index  $j$  is implied on the right-hand side, while the index  $i$  is free to vary over  $x$ ,  $y$ , or  $z$ .

In terms of the point particle acceleration,  $\mathbf{a}$ , and the hydrodynamic volume force  $\boldsymbol{\Sigma} \equiv \nabla \cdot \boldsymbol{\sigma}$  defined in (6.3.4), Cauchy's equation of motion takes the simple form

$$\rho \mathbf{a} = \boldsymbol{\Sigma} + \rho \mathbf{g} \quad (6.3.14)$$

for an incompressible or compressible fluid.

#### *Eulerian form*

Using equations (2.8.11) and (6.2.16), we derive two alternative forms of (6.3.12) involving derivatives with respect to time and position in space,

$$\rho \left( \frac{\partial \mathbf{u}}{\partial t} + \mathbf{u} \cdot \nabla \mathbf{u} \right) = \nabla \cdot \boldsymbol{\sigma} + \rho \mathbf{g} \quad (6.3.15)$$



$$\begin{aligned} \rho \left( \frac{\partial u_x}{\partial t} + u_x \frac{\partial u_x}{\partial x} + u_y \frac{\partial u_x}{\partial y} + u_z \frac{\partial u_x}{\partial z} \right) &= \frac{\partial \sigma_{xx}}{\partial x} + \frac{\partial \sigma_{yx}}{\partial y} + \frac{\partial \sigma_{zx}}{\partial z} + \rho g_x \\ \rho \left( \frac{\partial u_y}{\partial t} + u_x \frac{\partial u_y}{\partial x} + u_y \frac{\partial u_y}{\partial y} + u_z \frac{\partial u_y}{\partial z} \right) &= \frac{\partial \sigma_{xy}}{\partial x} + \frac{\partial \sigma_{yy}}{\partial y} + \frac{\partial \sigma_{zy}}{\partial z} + \rho g_y \\ \rho \left( \frac{\partial u_z}{\partial t} + u_x \frac{\partial u_z}{\partial x} + u_y \frac{\partial u_z}{\partial y} + u_z \frac{\partial u_z}{\partial z} \right) &= \frac{\partial \sigma_{xz}}{\partial x} + \frac{\partial \sigma_{yz}}{\partial y} + \frac{\partial \sigma_{zz}}{\partial z} + \rho g_z \end{aligned}$$

**Table 6.3.1** The Cartesian components of the equation of motion involving the point particle momentum, the hydrodynamic volume force, and the body force.

and

$$\frac{\partial(\rho \mathbf{u})}{\partial t} + \nabla \cdot (\rho \mathbf{u} \otimes \mathbf{u}) = \nabla \cdot \boldsymbol{\sigma} + \rho \mathbf{g}. \quad (6.3.16)$$

Both equations apply for incompressible as well as compressible fluids.

Explicitly, the three scalar components of (6.3.15) are given in Table 6.3.1. The terms enclosed by the parentheses on the left-hand sides are the Cartesian components of the point particle acceleration. The right-hand sides include the Cartesian components of the volume force due to the hydrodynamic stresses and the components of the body force.

### 6.3.4 Evolution equations

Given the instantaneous velocity and stress fields,  $\mathbf{u}$  and  $\boldsymbol{\sigma}$ , we can evaluate the right-hand sides of (6.3.12) and (6.3.15), as well as the second term on the left-hand side of (6.3.15), and thereby compute the rates of change  $D\mathbf{u}/Dt$  and  $\partial\mathbf{u}/\partial t$ . This observation suggests that the equation of motion (6.3.12) is, in fact, an evolution equation for the point particle velocity, whereas equation (6.3.15) is an evolution equation for the velocity at a fixed point in the flow.

A similar evolution equation for the density was derived in Chapter 2 on the basis of the continuity equation, as shown in (2.7.28). The evolution equations for the density and velocity originate from two fundamental physical laws: mass conservation, and Newton's second law of motion for a deformable medium.

### 6.3.5 Cylindrical polar coordinates

In the cylindrical polar coordinates defined in Figure 1.3.2, the hydrodynamic volume force defined in equation (6.3.4) is resolved into corresponding components,

$$\boldsymbol{\Sigma} = \Sigma_x \mathbf{e}_x + \Sigma_\sigma \mathbf{e}_\sigma + \Sigma_\varphi \mathbf{e}_\varphi. \quad (6.3.17)$$

(a)

$$\Sigma_x = \frac{\partial \sigma_{xx}}{\partial x} + \frac{1}{\sigma} \frac{\partial(\sigma \sigma_{\sigma x})}{\partial \sigma} + \frac{1}{\sigma} \frac{\partial \sigma_{\varphi x}}{\partial \varphi}, \quad \Sigma_\sigma = \frac{\partial \sigma_{x\sigma}}{\partial x} + \frac{1}{\sigma} \frac{\partial(\sigma \sigma_{\sigma\sigma})}{\partial \sigma} + \frac{1}{\sigma} \frac{\partial \sigma_{\varphi\sigma}}{\partial \varphi} - \frac{1}{\sigma} \sigma_{\varphi\varphi}$$

$$\Sigma_\varphi = \frac{\partial \sigma_{x\varphi}}{\partial x} + \frac{1}{\sigma^2} \frac{\partial(\sigma^2 \sigma_{\varphi\sigma})}{\partial \sigma} + \frac{1}{\sigma} \frac{\partial \sigma_{\varphi\varphi}}{\partial \varphi}$$

(b)

$$\Sigma_r = \frac{1}{r^2} \frac{\partial(r^2 \sigma_{rr})}{\partial r} + \frac{1}{r \sin \theta} \frac{\partial(\sigma_{r\theta} \sin \theta)}{\partial \theta} + \frac{1}{r \sin \theta} \frac{\partial \sigma_{\varphi r}}{\partial \varphi} - \frac{\sigma_{\theta\theta} + \sigma_{\varphi\varphi}}{r}$$

$$\Sigma_\theta = \frac{1}{r^2} \frac{\partial(r^2 \sigma_{r\theta})}{\partial r} + \frac{1}{r \sin \theta} \frac{\partial(\sigma_{\theta\theta} \sin \theta)}{\partial \theta} + \frac{1}{r \sin \theta} \frac{\partial \sigma_{\varphi\theta}}{\partial \varphi} + \frac{\sigma_{r\theta} - \sigma_{\varphi\varphi} \cot \theta}{r}$$

$$\Sigma_\varphi = \frac{1}{r^2} \frac{\partial(r^2 \sigma_{r\varphi})}{\partial r} + \frac{1}{r} \frac{\partial \sigma_{\theta\varphi}}{\partial \theta} + \frac{1}{r \sin \theta} \frac{\partial \sigma_{\varphi\varphi}}{\partial \varphi} + \frac{\sigma_{r\varphi} + 2 \sigma_{\theta\varphi} \cot \theta}{r}$$

(c)

$$\Sigma_r = \frac{1}{r} \frac{\partial(r \sigma_{rr})}{\partial r} + \frac{1}{r} \frac{\partial \sigma_{\theta r}}{\partial \theta} - \frac{1}{r} \sigma_{\theta\theta}, \quad \Sigma_\theta = \frac{1}{r^2} \frac{\partial(r^2 \sigma_{r\theta})}{\partial r} + \frac{1}{r} \frac{\partial \sigma_{\theta\theta}}{\partial \theta}$$

**Table 6.3.2** Components of the hydrodynamic volume force in terms of corresponding stress components in (a) cylindrical, (b) spherical, and (c) plane polar coordinates.

Using the rules of coordinate transformation and the chain rule of differentiation, we derive the expressions shown in [Table 6.3.2\(a\)](#).

### Equation of motion

The cylindrical polar components of the equation of motion are

$$\rho a_x = \Sigma_x + \rho g_x, \quad \rho a_\sigma = \Sigma_\sigma + \rho g_\sigma, \quad \rho a_\varphi = \Sigma_\varphi + \rho g_\varphi, \quad (6.3.18)$$

where  $a_x$ ,  $a_\sigma$ , and  $a_\varphi$  are the cylindrical polar components of the point particle acceleration given in equations (2.8.16). Using the alternative expressions (2.8.17), we obtain

$$\rho \frac{Du_x}{Dt} = \Sigma_x + \rho g_x, \quad \rho \frac{Du_\sigma}{Dt} = \rho \frac{u_\varphi^2}{\sigma} + \Sigma_\sigma + \rho g_\sigma,$$

$$\rho \frac{Du_\varphi}{Dt} = -\rho \frac{u_\sigma u_\varphi}{\sigma} + \Sigma_\varphi + \rho g_\varphi. \quad (6.3.19)$$

These equations apply for incompressible as well as compressible fluids.

### Centrifugal force

The first term on the right-hand side of the second equation in (6.3.19),  $\rho u_\varphi^2/\sigma$ , expresses an effective volume force in the radial ( $\sigma$ ) direction due to fluid motion in the azimuthal ( $\varphi$ ) direction, known as the centrifugal force. A centrifugal force arises in the flow generated by the rotation of a solid circular cylinder about its axis in a viscous liquid, as will be discussed in Section 7.5.

### Coriolis force

The negative of the first term on the right-hand side of third equation in (6.3.19),  $\rho u_\sigma u_\varphi/\sigma$ , expresses an effective force in the azimuthal ( $\varphi$ ) direction, known as the Coriolis force, arising when flow occurs in both the  $\sigma$  and  $\varphi$  directions. A Coriolis force is established in the flow due to a spinning circular disk immersed in a liquid.

### 6.3.6 Spherical polar coordinates

In the spherical polar coordinates defined in Figure 1.3.3, the hydrodynamic volume force defined in equation (6.3.4) is described as

$$\Sigma = \Sigma_r \mathbf{e}_r + \Sigma_\theta \mathbf{e}_\theta + \Sigma_\varphi \mathbf{e}_\varphi. \quad (6.3.20)$$

Using the rules of coordinate transformation and the chain rule of differentiation, we derive the expressions shown in Table 6.3.2(b).

The spherical polar components of the equation of motion are

$$\rho a_r = \Sigma_r + \rho g_r, \quad \rho a_\theta = \Sigma_\theta + \rho g_\theta, \quad \rho a_\varphi = \Sigma_\varphi + \rho g_\varphi, \quad (6.3.21)$$

where  $a_r$ ,  $a_\theta$ , and  $a_\varphi$  are the spherical polar components of the point particle acceleration given in (2.8.19).

### 6.3.7 Plane polar coordinates

In the plane polar coordinates defined in Figure 1.3.4, the hydrodynamic volume force defined in equation (6.3.4) is described as

$$\Sigma = \Sigma_r \mathbf{e}_r + \Sigma_\theta \mathbf{e}_\theta. \quad (6.3.22)$$

Using the coordinate transformation rules and the chain rule of differentiation, we derive the expressions shown in table 6.3.2(c).

The plane polar components of the equation of motion are

$$\rho a_r = \Sigma_r + \rho g_r, \quad \rho a_\theta = \Sigma_\theta + \rho g_\theta, \quad (6.3.23)$$

where  $a_r$  and  $a_\theta$  are the plane polar components of the point particle acceleration given by the expressions in (2.8.22). Alternative expressions are

$$\rho \frac{Du_r}{Dt} = \rho \frac{u_\theta^2}{r} + \Sigma_r + \rho g_r, \quad \rho \frac{Du_\theta}{Dt} = -\rho \frac{u_r u_\theta}{r} + \Sigma_\theta + \rho g_\theta, \quad (6.3.24)$$

involving, respectively, the centrifugal force and the negative of the Coriolis force on the right-hand sides, where  $D/Dt$  is the material derivative.

### 6.3.8 Vortex force

Returning to equation (6.3.15), we use identity (2.8.29),

$$\mathbf{u} \cdot \nabla \mathbf{u} = \frac{1}{2} \nabla u^2 - \mathbf{u} \times \boldsymbol{\omega}, \quad (6.3.25)$$

and obtain an alternative form of the equation of motion,

$$\rho \left( \frac{\partial \mathbf{u}}{\partial t} + \frac{1}{2} \nabla u^2 + \boldsymbol{\omega} \times \mathbf{u} \right) = \nabla \cdot \boldsymbol{\sigma} + \rho \mathbf{g}, \quad (6.3.26)$$

where

$$u^2 \equiv u_x^2 + u_y^2 + u_z^2 \quad (6.3.27)$$

is the square of the magnitude of the velocity. The third term on the left-hand side of (6.3.26),

$$\rho \boldsymbol{\omega} \times \mathbf{u}, \quad (6.3.28)$$

represents a vortex force established when the vorticity vector is not parallel to the velocity vector; otherwise, their cross product is identically zero. In a Beltrami flow, the vorticity vector is parallel to the velocity vector at every point and the vortex force is identically zero.

### 6.3.9 Summary of governing equation

In summary, the flow of an incompressible or compressible fluid is governed by the continuity equation (2.7.13),

$$\frac{\partial \rho}{\partial t} + \nabla \cdot (\rho \mathbf{u}) = 0, \quad (6.3.29)$$

and Cauchy's equation of motion expressed by (6.3.15) or (6.3.16). The Cauchy stress tensor is defined in terms of the velocity and the pressure by means of a constitutive equation, as discussed in Chapter 4. The five unknowns include the three velocity components,  $u_x$ ,  $u_y$ ,  $u_z$ , the density,  $\rho$ , and the pressure,  $p$ .

The continuity equation and the three components of the equation of motion provide us with four equations. In the case of incompressible fluids, a fifth equation is provided by the idealized incompressibility condition,  $D\rho/Dt = 0$ . In the case of compressible fluids, a fifth equation relating the density to the pressure is provided by thermodynamics, as shown in (4.7.23) for isentropic flow.

### 6.3.10 Accelerating frame of reference

The equation of motion is valid for a stationary frame of reference where Newton's second law of motion applies. Suppose that the Cartesian axes translate with velocity  $\mathbf{V}(t)$  in the absence of rotation. The point particle acceleration in the stationary frame is

$$\mathbf{a}^{\text{stationary}} = \mathbf{a} + \frac{d\mathbf{V}}{dt}. \quad (6.3.30)$$

Substituting this expression in the equation of motion (6.3.14) and rearranging, we derive the equation

$$\rho \mathbf{a} = \boldsymbol{\Sigma} + \rho \mathbf{g} - \rho \frac{d\mathbf{V}}{dt}. \quad (6.3.31)$$

The last term on the right-hand side represents a fictitious inertial acceleration force. A more general equation can be written to describe fluid motion in a frame of reference that undergoes simultaneous steady or unsteady translation and rotation.<sup>2</sup>

## PROBLEMS

### 6.3.1 Beltrami flow

Explain why a two-dimensional or axisymmetric flow cannot be a Beltrami flow.

### 6.3.2 Free fall

A bucket of fluid is moving in free gravitational fall. Write the equation of motion in a frame of reference attached to the bucket.

## 6.4 Euler and Bernoulli equations

Euler's equation arises from the equation of motion (6.3.12) by substituting the simplest possible constitutive equation for the stress tensor describing an ideal fluid, expressed by equation (4.6.19). Considering the individual components of the volume force  $\boldsymbol{\Sigma}$  given in (6.3.5), we obtain

$$\boldsymbol{\Sigma} \equiv \nabla \cdot \boldsymbol{\sigma} = -\nabla p, \quad (6.4.1)$$

that is,

$$\boldsymbol{\Sigma} = -\frac{\partial p}{\partial x} \mathbf{e}_x - \frac{\partial p}{\partial y} \mathbf{e}_y - \frac{\partial p}{\partial z} \mathbf{e}_z, \quad (6.4.2)$$

where  $p$  is the pressure. Cauchy's equation of motion (6.3.12) then reduces to Euler's equation of motion,

$$\rho \frac{D\mathbf{u}}{Dt} = -\nabla p + \rho \mathbf{g}. \quad (6.4.3)$$

<sup>2</sup>Pozrikidis, C. (2011) *Introduction to Theoretical and Computational Fluid Dynamics*, Second Edition, Oxford University Press.

$$\begin{aligned}\rho \left( \frac{\partial u_x}{\partial t} + u_x \frac{\partial u_x}{\partial x} + u_y \frac{\partial u_x}{\partial y} + u_z \frac{\partial u_x}{\partial z} \right) &= -\frac{\partial p}{\partial x} + \rho g_x \\ \rho \left( \frac{\partial u_y}{\partial t} + u_x \frac{\partial u_y}{\partial x} + u_y \frac{\partial u_y}{\partial y} + u_z \frac{\partial u_y}{\partial z} \right) &= -\frac{\partial p}{\partial y} + \rho g_y \\ \rho \left( \frac{\partial u_z}{\partial t} + u_x \frac{\partial u_z}{\partial x} + u_y \frac{\partial u_z}{\partial y} + u_z \frac{\partial u_z}{\partial z} \right) &= -\frac{\partial p}{\partial z} + \rho g_z\end{aligned}$$

**Table 6.4.1** The three Cartesian components of Euler's equation describing the motion of a fluid in the absence of viscous forces.

The associated Eulerian form is

$$\rho \left( \frac{\partial \mathbf{u}}{\partial t} + \mathbf{u} \cdot \nabla \mathbf{u} \right) = -\nabla p + \rho \mathbf{g}. \quad (6.4.4)$$

The three Cartesian components of (6.4.4) are shown in Table 6.4.1. Euler's equation applies for incompressible as well as compressible fluids.

### Polar coordinates

The cylindrical, spherical, and plane polar components of Euler's equation follow readily from equations (6.3.18), (6.3.21), and (6.3.23), using the constitutive equations given in Tables 4.7.1–Table 4.7.3 for vanishing fluid viscosity.

### Vortex force

Using identity (2.8.29), repeated below for convenience,

$$\mathbf{u} \cdot \nabla \mathbf{u} = \frac{1}{2} \nabla u^2 - \mathbf{u} \times \boldsymbol{\omega}, \quad (6.4.5)$$

we derive an alternative form of Euler's equation involving the vortex force,

$$\rho \left( \frac{\partial \mathbf{u}}{\partial t} + \frac{1}{2} \nabla u^2 - \mathbf{u} \times \boldsymbol{\omega} \right) = -\nabla p + \rho \mathbf{g}, \quad (6.4.6)$$

where

$$u^2 \equiv u_x^2 + u_y^2 + u_z^2 \quad (6.4.7)$$

is the square of the magnitude of the velocity.

## 6.4.1 Boundary conditions

Euler's equation is a first-order differential equation for the velocity and pressure in the domain of flow. To compute a solution, we require one scalar boundary condition or two

scalar continuity or jump conditions for the velocity or pressure over each boundary of the flow.

#### *Impermeable surfaces*

Over an impermeable surface, we require the no-penetration condition requiring that the normal component of the fluid velocity matches the normal component of the boundary velocity.

#### *Free surfaces*

Over a free surface, we require that the pressure is equal to the ambient pressure increased or decreased by an amount that is equal to the product of the surface tension and twice the local mean curvature.

#### *Fluid interfaces*

Over a fluid interface, we require a kinematic and a dynamic continuity or jump condition. The kinematic condition requires that the normal component of the fluid velocity is continuous across the interface. The dynamic condition requires that the pressure undergoes a discontinuity by an amount that is equal to the product of the surface tension and twice the local mean curvature.

### **6.4.2 Irrotational flow**

The third term on the left-hand side of Euler's equation (6.4.6) disappears in the case of irrotational flow, since  $\boldsymbol{\omega} = \mathbf{0}$  throughout the domain of flow. Expressing the velocity as the gradient of a velocity potential,  $\phi$ , as shown in equation (3.2.6) and more explicitly in equations (3.2.19),

$$\mathbf{u} = \nabla\phi, \quad (6.4.8)$$

we find that Euler's equation (6.4.6) takes the form

$$\rho \left( \frac{\partial \nabla\phi}{\partial t} + \frac{1}{2} \nabla u^2 \right) = -\nabla p + \rho \mathbf{g}. \quad (6.4.9)$$

The order of time and space differentiation in the gradient of the potential can be switched in the first term on the left-hand side.

The acceleration of gravity can be expressed as the gradient of the scalar  $v \equiv \mathbf{g} \cdot \mathbf{x}$ ,

$$\mathbf{g} = \nabla v = \nabla(\mathbf{g} \cdot \mathbf{x}) = \nabla(g_x x + g_y y + g_z z). \quad (6.4.10)$$

Substituting this expression into (6.4.9), assuming that the density is uniform throughout the domain of flow, and collecting all terms under the gradient, we find that

$$\nabla \left( \frac{\partial \phi}{\partial t} + \frac{1}{2} u^2 + \frac{p}{\rho} - \mathbf{g} \cdot \mathbf{x} \right) = \mathbf{0}. \quad (6.4.11)$$

The curl of the left-hand side is identically zero at every point in the flow.

### *Bernoulli's equation for irrotational flow*

Since all spatial derivatives of the scalar quantity enclosed by the parentheses on the left-hand side of (6.4.11) are zero, the quantity must be independent of position, although it may change in time. Euler's equation for irrotational flow then provides us with Bernoulli's equation describing the irrotational flow of a uniform-density fluid,

$$\frac{\partial \phi}{\partial t} + \frac{1}{2} u^2 + \frac{p}{\rho} - \mathbf{g} \cdot \mathbf{x} = c(t), \quad (6.4.12)$$

where  $c(t)$  is an unspecified and typically inconsequential function of time.

### *Evolution of the velocity potential*

Bernoulli's equation (6.4.12) can be regarded as an evolution equation for the harmonic potential. Given the instantaneous velocity and pressure fields, we can evaluate the second, third, and fourth terms on the left-hand side, compute the time derivative  $\partial\phi/\partial t$ , and advance the potential over a small period of time elapsed.

The last term,  $c(t)$ , causes the potential to increase or decrease uniformly by the same rate throughout the domain of flow. However, because the velocity is computed by taking derivatives of the potential with respect to the spatial coordinates, this uniform change is inconsequential to the velocity.

### *Lagrangian form*

When a flow is bounded by a free surface where the pressure is prescribed on one side, it is beneficial to convert the Eulerian time derivative  $\partial\phi/\partial t$  on the left-hand side of (6.4.12) to the material derivative,  $D\phi/Dt$ . Expressing the velocity as the gradient of the potential,  $\mathbf{u} = \nabla\phi$ , we obtain

$$\frac{D\phi}{Dt} \equiv \frac{\partial\phi}{\partial t} + \mathbf{u} \cdot \nabla\phi = \frac{\partial\phi}{\partial t} + \mathbf{u} \cdot \mathbf{u} = \frac{\partial\phi}{\partial t} + u^2, \quad (6.4.13)$$

where

$$u^2 \equiv u_x^2 + u_y^2 + u_z^2 \quad (6.4.14)$$

is the square of the magnitude of the velocity. Combining equations (6.4.12) and (6.4.13), we obtain

$$\frac{D\phi}{Dt} = \frac{1}{2} u^2 - \frac{p}{\rho} + \mathbf{g} \cdot \mathbf{x} - c(t), \quad (6.4.15)$$

which provides us with the rate of change of the potential following a point particle according to Bernoulli's equation for irrotational flow.



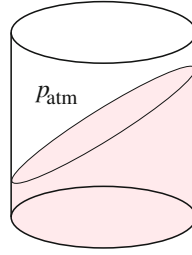


**Figure 6.4.1** Irrotational flow due to the sloshing of a fluid in a container. Bernoulli's equation provides us with an evolution equation for the potential following the motion of point particles distributed over the free surface.

### Fluid sloshing in a container

As an application, we consider the sloshing of a fluid inside a container, as illustrated in Figure 6.4.1. The pressure at the free surface on the side of the liquid,  $p_{fs}$ , is related to the ambient pressure,  $p_{atm}$ , by the dynamic boundary condition

$$p_{fs} = p_{atm} + \gamma 2 \kappa_m, \quad (6.4.16)$$

where  $\gamma$  is the surface tension and  $\kappa_m$  is the mean curvature of the free surface.

Applying equation (6.4.15) at a point in the free surface and using equation (6.4.16), we derive an expression for the rate of change of the potential following a point particle at the free surface,

$$\frac{D\phi}{Dt} = \frac{1}{2} u^2 - \frac{p_{atm} + \gamma 2 \kappa_m}{\rho} + \mathbf{g} \cdot \mathbf{x} - c(t). \quad (6.4.17)$$

Integrating this equation in time by following the motion of interfacial point particles provides us with a boundary condition for the potential over the free surface.

### Steady irrotational flow

The time derivative of the potential on the left-hand side of (6.4.12) disappears at steady state, yielding the best known version of Bernoulli's equation,

$$\frac{1}{2} u^2 + \frac{p}{\rho} - \mathbf{g} \cdot \mathbf{x} = c(t). \quad (6.4.18)$$

The time-dependent function  $c(t)$  on the right-hand side accounts for a possible uniform change in the pressure throughout the domain of flow.

The three terms on the left-hand side of (6.4.18) express, respectively, the kinetic energy, the potential energy due to the pressure, and the potential energy due to the body force, all three per unit mass of the fluid. Bernoulli's equation requires that the sum of the three energies is the same at every point in the flow.

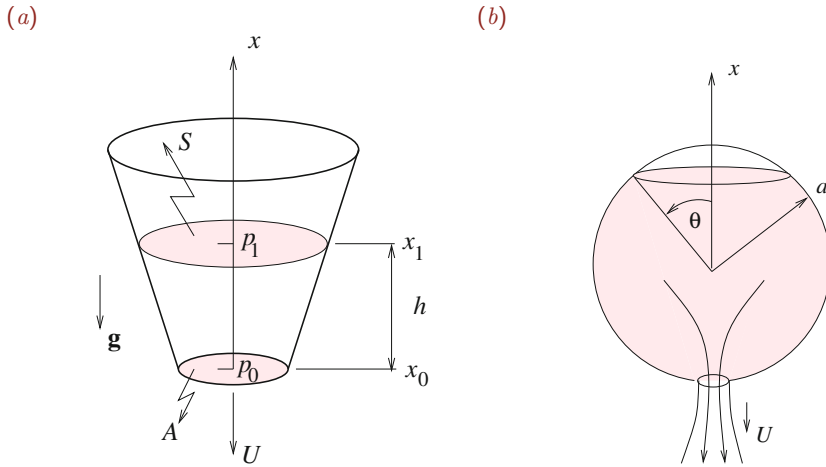


**Figure 6.4.2** Illustration of the gravitational drainage of a fluid from a (a) conical or (b) spherical tank. The exit velocity can be computed from Bernoulli's equation for irrotational flow, resulting in Torricelli's law.

Bernoulli's equation allows us to perform approximate engineering analysis of a broad class of internal and external irrotational flows, subject to the underlying assumptions. Examples are discussed in the remainder of this section.

### 6.4.3 Torricelli's law

Consider the gravitational drainage of a fluid from a tank, as illustrated in Figure 6.4.2. If the rate of drainage is sufficiently slow, the flow can be assumed to be in a quasi-steady state. This means that the magnitude of the time derivative of the scalar potential is small compared to the rest of the terms in the unsteady Bernoulli equation (6.4.12), and the steady version of Bernoulli's equation (6.4.18) can be employed.

To compute the velocity at the point of drainage,  $U$ , we evaluate the left-hand side of (6.4.18) first at the free surface and then at the point of drainage, and equate the two expressions. Since the velocity at the free surface is small compared to the drainage velocity, it can be set to zero to leading-order approximation, yielding

$$\frac{1}{2} U^2 + \frac{p_0}{\rho} + g x_0 = \frac{p_1}{\rho} + g x_1, \quad (6.4.19)$$

where the pressures  $p_0$  and  $p_1$  and the elevations  $x_0$  and  $x_1$ , are defined in Figure 6.4.2(a). Rearranging, we find that

$$U = \left( 2 \frac{\Delta p}{\rho} + 2gh \right)^{1/2}, \quad (6.4.20)$$

where  $h = x_1 - x_0$  is the liquid height inside the container and  $\Delta p = p_1 - p_0$ .

In the case of an open tank, the pressure at the free surface and the pressure at the point of drainage are equal to the ambient atmospheric pressure. Setting  $\Delta p = 0$ , and derive Torricelli's law expressed by

$$U = \sqrt{2gh}, \quad (6.4.21)$$

which also describes the velocity of a rigid body in free gravitational fall.

### Drainage time

The expression for the velocity in terms of the liquid height,  $h$ , can be used to compute the time it takes for a fluid to drain from a tank with a specified geometry,  $t_{\text{drain}}$ . During a small period of time,  $dt$ , the volume of liquid in the tank decreases by

$$dV = S(x) dh, \quad (6.4.22)$$

where  $S(h)$  is the tank cross-sectional area. Setting this change in volume equal to  $-UA dt$ , where  $A$  is the cross-sectional area of the drainage hole, and substituting Torricelli's law, we obtain

$$S(h) dh = -\sqrt{2gh} A dt, \quad (6.4.23)$$

which can be rearranged into

$$\frac{dt}{dh} = -\frac{1}{A} \frac{S(h)}{\sqrt{2gh}}. \quad (6.4.24)$$

Integrating, we obtain an expression for the drainage time,

$$t_{\text{drain}} = \frac{1}{A} \int_0^{h_0} \frac{S(h)}{\sqrt{2gh}} dh, \quad (6.4.25)$$

where  $h_0$  is the initial height of the liquid in the container.

### Cylindrical tank

In the case of a cylindrical tank with arbitrary cross-section, the cross-sectional area is constant,  $S(h) \equiv B$ , yielding

$$t_{\text{drain}} = \frac{B}{A} \frac{1}{\sqrt{2g}} \int_0^{h_0} \frac{1}{\sqrt{h}} dh = \frac{B}{A} \left(2 \frac{h_0}{g}\right)^{1/2}. \quad (6.4.26)$$

This functional form could have been predicted at the outset on the basis of dimensional analysis. In the case of a vertical barrel,  $B = \pi b^2$ , where  $b$  is the barrel radius.

### Conical container

In the case of a conical container illustrated in [Figure 6.4.2\(a\)](#), the radius of the cross-section at height  $h$  is approximately  $r \simeq r_0 h/h_0$ , where  $r_0$  is the radius of the cross-section at the initial height,  $h_0$ . Setting  $S(h) = \pi r^2$ , we obtain

$$t_{\text{drain}} = \frac{B_0}{Ah_0^2} \frac{1}{\sqrt{2g}} \int_0^{h_0} h^{3/2} dh, \quad (6.4.27)$$

where  $B_0 = \pi r_0^2$  is the cross-sectional area at height  $h_0$ , and the origin of the  $x$  axis has been set at the hole. Performing the integration, we obtain

$$t_{\text{drain}} = \frac{1}{5} \frac{B_0}{A} \left( 2 \frac{h_0}{g} \right)^{1/2}, \quad (6.4.28)$$

$B_0/A = (r_0/a)^2$ , and  $r_0$  is the hole radius. The drainage time is one fifth of that for the cylindrical container with cross-sectional area  $B = B_0$ .

### Spherical container

In the case of a spherical container of radius  $a$ , the height of the liquid can be parametrized by the meridional angle,  $\theta$ ,

$$h = (1 + \cos \theta) a, \quad (6.4.29)$$

as illustrated in [Figure 6.4.2\(b\)](#). The radius of the cross-section at height  $h$  is  $r = a \sin \theta$  and the corresponding cross-sectional area is  $S = \pi a^2 \sin^2 \theta$ . Substituting these expressions into the master equation (6.4.25), we obtain

$$t_{\text{drain}} = \frac{\pi a^2}{A} \left( \frac{b}{2g} \right)^{1/2} \int_{\pi}^{\alpha} \frac{\sin^2 \theta}{\sqrt{1 + \cos \theta}} (-\sin \theta) d\theta, \quad (6.4.30)$$

where  $\alpha$  is the initial meridional angle. In the case of a full spherical container,  $\alpha = 0$ ; in the case of a full hemispherical container,  $\alpha = \pi/2$ .

Substituting for convenience  $w = \cos \theta$ , we obtain

$$t_{\text{drain}} = \frac{\pi a^2}{A} \left( \frac{a}{2g} \right)^{1/2} \int_{-1}^{\cos \alpha} (1 - w) \sqrt{1 + \cos w} dw. \quad (6.4.31)$$

Recalling the indefinite integrals

$$\int \sqrt{1 + w} dw = \frac{2}{3} (1 + w)^{3/2} \quad (6.4.32)$$

and

$$\int w \sqrt{1 + w} dw = \frac{2}{15} (3w - 2) (1 + w)^{3/2}, \quad (6.4.33)$$

we obtain

$$t_{\text{drain}} = \frac{2}{15} \frac{\pi a^2}{A} \left( \frac{a}{2g} \right)^{1/2} (1 + \cos \alpha)^{3/2} (7 - 3 \cos \alpha). \quad (6.4.34)$$

In the case of a full spherical container,  $\cos \alpha = 1$ ; in the case of a full hemispherical container,  $\cos \alpha = 0$ .

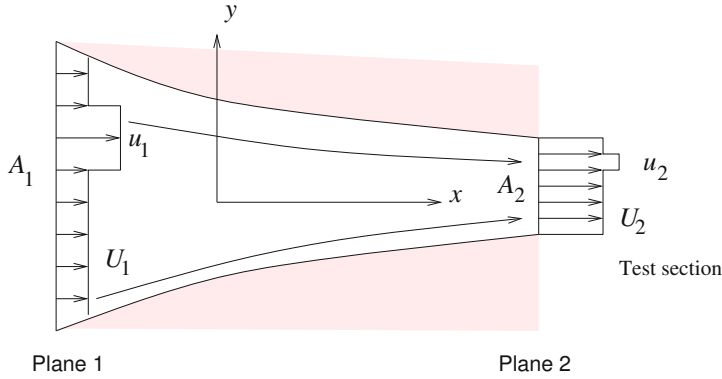


**Figure 6.4.3** Illustration of flow in a wind or water tunnel with a contraction that dampens small perturbations.

**6.4.4 Decay of perturbations in a wind or water tunnel**

Wind and water tunnels are used extensively in laboratory studies of high-speed flow. To obtain a desirable uniform velocity profile, the tunnel is designed with a smooth contraction upstream from a test section where measurement or observation takes place, as illustrated in Figure 6.4.3. Consider a small perturbation of the otherwise flat upstream velocity profile at plane 1, as illustrated in Figure 6.4.3. The pressure is nearly uniform over any cross-section along the contraction.

Applying Bernoulli’s equation (6.4.18) for the fluid outside or inside the perturbed region, and neglecting the effect of gravity, we find that

$$\frac{1}{2} U_1^2 + \frac{p_1}{\rho} = \frac{1}{2} U_2^2 + \frac{p_2}{\rho}, \quad \frac{1}{2} u_1^2 + \frac{p_1}{\rho} = \frac{1}{2} u_2^2 + \frac{p_2}{\rho}. \tag{6.4.35}$$

Combining these equations to eliminate the pressure and rearranging, we obtain

$$\frac{U_2 - u_2}{U_1 - u_1} = \frac{U_1 + u_1}{U_2 + u_2}. \tag{6.4.36}$$

Because the perturbation has been assumed small, the actual velocities,  $u_1$  and  $u_2$ , can be replaced with the unperturbed velocities  $U_1$  and  $U_2$  in the numerator and denominator of the fraction on the right-hand side of (6.4.36), yielding

$$\frac{U_2 - u_2}{U_1 - u_1} = \frac{U_1}{U_2}. \tag{6.4.37}$$

Now combining the approximate mass balance  $U_1 A_1 = U_2 A_2$  with equation (6.4.37) and rearranging, we obtain

$$\frac{1 - u_2/U_2}{1 - u_1/U_1} = \left(\frac{A_2}{A_1}\right)^2, \tag{6.4.38}$$

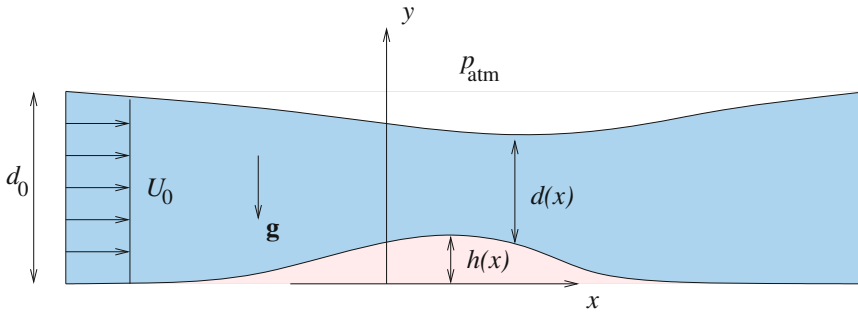


**Figure 6.4.4** Irrotational free-surface flow of a horizontal stream over a hump.

which shows that the relative magnitude of the perturbation decays like the square of the contraction ratio,  $A_2/A_1$ , thereby confirming that the contraction promotes a uniform velocity profile.

### 6.4.5 Flow of a horizontal stream over a hump

In the third application, we consider steady two-dimensional irrotational flow of a horizontal stream over a gently sloped hump, called the Venturi flume, as illustrated in [Figure 6.4.4](#). The free surface is located at

$$y = h(x) + d(x), \quad (6.4.39)$$

where  $h(x)$  is the height of the hump and  $d(x)$  is the depth of the stream. As  $x$  tends to infinity on either side,  $h(x)$  tends to zero. The profile of the streamwise velocity is assumed to be uniform across the stream, that is,  $u_x = u(x)$ .

Applying Bernoulli's equation (6.4.18) first at a point at the free surface located far upstream and then at an arbitrary point at the free surface, neglecting the  $y$  component of the free-surface velocity and the pressure drop across the free surface due to surface tension, and noting that the gravitational acceleration vector is given by  $\mathbf{g} = (0, -g)$ , we obtain

$$\frac{1}{2} U_0^2 + \frac{p_{\text{atm}}}{\rho} + g d_0 = \frac{1}{2} u^2(x) + \frac{p_{\text{atm}}}{\rho} + g (h(x) + d(x)), \quad (6.4.40)$$

where  $U_0$  is the upstream velocity and  $d_0 \equiv d(x = -\infty)$  is the upstream depth. Combining the mass conservation equation

$$U_0 d_0 = u(x) d(x) \quad (6.4.41)$$

with equation (6.4.40) to eliminate  $u(x)$ , and rearranging the resulting expression, we derive a cubic equation for the scaled layer depth  $\hat{d}(x) \equiv d(x)/d_0$ ,

$$\hat{d}^3(x) + \hat{d}^2(x) (\hat{h}(x) - 1 - \frac{1}{2} \text{Fr}^2) + \frac{1}{2} \text{Fr}^2 = 0, \quad (6.4.42)$$

where  $\widehat{h}(x) \equiv h(x)/d_0$  is the scaled height of the hump. We have introduced the dimensionless ratio

$$\text{Fr} \equiv \frac{U_0}{\sqrt{g d_0}}, \quad (6.4.43)$$

expressing the relative magnitude of inertial and gravitational forces, called the Froude number.

In practice, the Venturi flume is used to deduce the flow rate from measurements of the deflection of the free surface from the horizontal position. As the Froude number tends to zero, gravitational forces dominate and equation (6.4.42) has the obvious solution  $\widehat{d}(x) = 1 - \widehat{h}(x)$ , which shows that the free surface tends to become flat. As the Froude number tends to infinity, inertial forces dominate and equation (6.4.42) has an obvious solution,  $\widehat{d}(x) = 1$ , which shows that the depth of the stream remains constant and the free surface follows the topography of the hump. Intermediate values of the Froude number yield free surface profiles with a downward deflection (Problem 6.4.6).

#### 6.4.6 Steady rotational flow

We return to Euler's equation (6.4.6) and consider a rotational flow at steady state. The time derivative on the left-hand side vanishes, yielding

$$\frac{1}{2} \nabla u^2 - \mathbf{u} \times \boldsymbol{\omega} = -\frac{1}{\rho} \nabla p + \mathbf{g}, \quad (6.4.44)$$

where

$$u^2 \equiv u_x^2 + u_y^2 + u_z^2 \quad (6.4.45)$$

is the square of the magnitude of the velocity. The  $x$  component of equation (6.4.44) reads

$$\frac{1}{2} \frac{\partial u^2}{\partial x} - u_y \omega_z + u_z \omega_y = -\frac{1}{\rho} \frac{\partial p}{\partial x} + g_x. \quad (6.4.46)$$

Similar equations can be written for the  $y$  and  $z$  components.

Next, we place the origin of the Cartesian axes at a point in the fluid, identify the streamline that passes through that point, and orient the  $x$  axis tangentially to the streamline and thus parallel to the local velocity, as shown in [Figure 6.4.5](#). By design, the  $y$  and  $z$  velocity components are zero at the origin; consequently, the second and third terms on the left-hand side of equation (6.4.46) vanish. Taking advantage of these simplifications, we derive the reduced form

$$\frac{\partial}{\partial x} \left( \frac{1}{2} u^2 + \frac{p}{\rho} - g_x x \right) = 0, \quad (6.4.47)$$

where the left-hand side is evaluated at the origin.

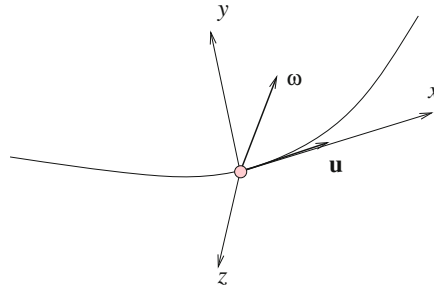


**Figure 6.4.5** A system of Cartesian coordinates with the  $x$  axis tangential to a streamline is used to derive Bernoulli's equation for steady rotational flow, given in equation (6.4.48).

Equation (6.4.47) states that the rate of change of the quantity enclosed by the parentheses on the left-hand side with respect to distance along the streamline is zero. Consequently, the quantity enclosed by the parentheses must remain constant along the streamline,

$$\frac{1}{2} u^2 + \frac{p}{\rho} - \mathbf{g} \cdot \mathbf{x} = f(x, y, z), \quad (6.4.48)$$

where the function  $f(x, y, z)$  remains constant along a streamline. In a two-dimensional or axisymmetric flow,  $f(x, y, z)$  is a function of the stream function,  $\psi$ , which, by definition, is constant along a streamline.

#### 6.4.7 Flow with uniform vorticity

The velocity field,  $\mathbf{u}$ , of a two-dimensional flow with uniform vorticity in the  $xy$  plane,  $\omega_z = \Omega$ , can be resolved into (a) the velocity field,  $\mathbf{v}$ , of a simple two-dimensional flow with uniform vorticity  $\Omega$ , and (b) the velocity field of a potential flow expressed by a harmonic potential  $\phi$ , such that

$$\mathbf{u} = \mathbf{v} + \nabla\phi. \quad (6.4.49)$$

One example of a simple flow is simple shear flow with velocity

$$v_x = -\Omega y, \quad v_y = 0. \quad (6.4.50)$$

A second example is flow expressing rigid-body rotation with velocity

$$v_x = -\frac{1}{2} \Omega y, \quad v_y = \frac{1}{2} \Omega x. \quad (6.4.51)$$

Using this decomposition, we derive Bernoulli's equation

$$\frac{\partial\phi}{\partial t} + \frac{1}{2} u^2 + \frac{p}{\rho} - \mathbf{g} \cdot \mathbf{x} + \Omega\psi = c(t), \quad (6.4.52)$$

where  $\psi$  is the stream function and  $u = |\mathbf{u}|$  is the magnitude of the velocity (Problem 6.4.2).



**PROBLEMS****6.4.1** *Flow through a sudden enlargement*

Consider the flow through a sudden enlargement depicted in [Figure 6.2.1](#). Use Bernoulli's equation to compute the rise in pressure,  $p_2 - p_1$ . Compare your answer to that shown in equation (6.2.28) obtained by an approximate integral momentum balance.

**6.4.2** *Flow with uniform vorticity*

(a) Derive Bernoulli's equation (6.4.52) for two-dimensional flow. (b) Derive a similar equation for axisymmetric flow where the azimuthal component of the vorticity,  $\omega_\varphi$ , is proportional to the distance from the axis of symmetry,  $\sigma$ .

**6.4.3** *Flow due to an unsteady point source or point vortex*

(a) Discuss whether the flow due to a two- or three-dimensional point source with time-dependent strength satisfies the Euler equation for inviscid flow. (b) Repeat (a) for a two-dimensional point vortex.

**6.4.4** *Force on a sphere in accelerating potential flow*

Consider an unsteady irrotational flow past a sphere that is held stationary in an accelerating stream along the  $x$  axis with velocity  $U_x(t)$ . The velocity potential and Cartesian components of the velocity are given in equations (3.6.13) and (3.6.14). Use Bernoulli's equation (6.4.12) to evaluate the pressure and then compute the force exerted on the sphere by evaluating the surface integral


$$\mathbf{F} = - \iint_{\text{sphere}} p \mathbf{n} \, dS, \quad (6.4.53)$$

where  $\mathbf{n} = \frac{1}{a}(x, y, z)$  is the unit vector normal to the sphere pointing into the fluid. Based on this result, compute the force exerted on a sphere that is held stationary in a non-accelerating steady flow. Discuss the physical relevance of the assumption of irrotational flow.

**6.4.5** *Drainage from a spheroidal tank*

(a) Derive a formula for the time it takes a liquid to drain completely from a vertical spheroidal tank with axes  $a$  and  $b$  through a small hole at the bottom, based on Torricelli's law. You may assume that the gas pressure is equal to the atmospheric pressure above the liquid in the tank.

(b) Repeat (a) for a horizontal spheroidal tank.

**6.4.6**  *Flow over a hump*

Consider the flow of a horizontal stream over a hump, as illustrated in [Figure 6.4.4](#). The height of the hump is described by the parabolic shape function

$$h(x) = h_0 (1 - \hat{x}^2) \quad (6.4.54)$$

for  $-1 \leq \hat{x} \leq 1$ , where  $h_0$  is the maximum height,  $\hat{x} \equiv x/a$  is the scaled distance from the midpoint, and  $a$  is the half-length of the hump. Substituting this profile into (6.4.42), we derive the equation

$$\hat{d}^3(x) + \hat{d}^2(x) \left( \frac{h_0}{d_0} (1 - \hat{x}^2) - 1 - \frac{1}{2} \text{Fr}^2 \right) + \frac{1}{2} \text{Fr}^2 = 0 \quad (6.4.55)$$

for  $-1 \leq \hat{x} \leq 1$ . Compute and plot the scaled layer depth  $\hat{d}$  against  $\hat{x}$  for  $h_0/d_0 = 0.01, 0.05, \text{ and } 0.10$ , and  $\text{Fr} = 0.01, 0.1, 10, \text{ and } 100$ . Discuss the free surface shapes.

## 6.5 The Navier–Stokes equation

The Navier–Stokes equation arises from the equation of motion (6.3.12) by substituting the constitutive equation for the stress tensor for an incompressible Newtonian fluid, given in (4.6.6). The hydrodynamic volume force for a fluid with uniform viscosity is given by

$$\Sigma \equiv \nabla \cdot \boldsymbol{\sigma} = \nabla \cdot (-p \mathbf{I} + \mu 2 \mathbf{E}) = -\nabla p + \mu 2 \nabla \cdot \mathbf{E}, \quad (6.5.1)$$

where  $\mathbf{I}$  is the identity matrix and  $\mathbf{E}$  is the rate-of-deformation tensor.

Working in index notation, we find that the  $i$ th component of twice the divergence of the rate-of-deformation tensor on the right-hand side is

$$2 \frac{\partial E_{ji}}{\partial x_j} = 2 \frac{\partial}{\partial x_j} \left[ \frac{1}{2} \left( \frac{\partial u_i}{\partial x_j} + \frac{\partial u_j}{\partial x_i} \right) \right], \quad (6.5.2)$$

where summation is implied over the repeated index  $j$ . Carrying out the differentiations, we obtain

$$2 \frac{\partial E_{ji}}{\partial x_j} = \frac{\partial^2 u_i}{\partial x_j \partial x_j} + \frac{\partial^2 u_j}{\partial x_j \partial x_i} = \frac{\partial^2 u_i}{\partial x_j \partial x_j} + \frac{\partial}{\partial x_i} \left( \frac{\partial u_j}{\partial x_j} \right). \quad (6.5.3)$$

Because the fluid has been assumed incompressible, the divergence of the velocity in the last term enclosed by the parentheses is zero. The penultimate term is the Laplacian of the  $i$ th component of the velocity,

$$\frac{\partial^2 u_i}{\partial x_j \partial x_j} = \frac{\partial^2 u_i}{\partial x^2} + \frac{\partial^2 u_i}{\partial y^2} + \frac{\partial^2 u_i}{\partial z^2} \equiv \nabla^2 u_i. \quad (6.5.4)$$

Using these results to simplify expression (6.5.1), we find that the hydrodynamic volume force is given by

$$\Sigma \equiv \nabla \cdot \boldsymbol{\sigma} = -\nabla p + \mu \nabla^2 \mathbf{u}. \quad (6.5.5)$$

Correspondingly, Cauchy's equation of motion (6.3.12) reduces to the Navier–Stokes equation,

$$\rho \frac{D\mathbf{u}}{Dt} = -\nabla p + \mu \nabla^2 \mathbf{u} + \rho \mathbf{g}, \quad (6.5.6)$$

$$\begin{aligned}\rho \left( \frac{\partial u_x}{\partial t} + u_x \frac{\partial u_x}{\partial x} + u_y \frac{\partial u_x}{\partial y} + u_z \frac{\partial u_x}{\partial z} \right) &= -\frac{\partial p}{\partial x} + \mu \left( \frac{\partial^2 u_x}{\partial x^2} + \frac{\partial^2 u_x}{\partial y^2} + \frac{\partial^2 u_x}{\partial z^2} \right) + \rho g_x \\ \rho \left( \frac{\partial u_y}{\partial t} + u_x \frac{\partial u_y}{\partial x} + u_y \frac{\partial u_y}{\partial y} + u_z \frac{\partial u_y}{\partial z} \right) &= -\frac{\partial p}{\partial y} + \mu \left( \frac{\partial^2 u_y}{\partial x^2} + \frac{\partial^2 u_y}{\partial y^2} + \frac{\partial^2 u_y}{\partial z^2} \right) + \rho g_y \\ \rho \left( \frac{\partial u_z}{\partial t} + u_x \frac{\partial u_z}{\partial x} + u_y \frac{\partial u_z}{\partial y} + u_z \frac{\partial u_z}{\partial z} \right) &= -\frac{\partial p}{\partial z} + \mu \left( \frac{\partial^2 u_z}{\partial x^2} + \frac{\partial^2 u_z}{\partial y^2} + \frac{\partial^2 u_z}{\partial z^2} \right) + \rho g_z\end{aligned}$$

**Table 6.5.1** Eulerian form of the three Cartesian components of the Navier–Stokes equation applicable to incompressible Newtonian fluids.

which is distinguished from Euler’s equation (6.4.3) by the presence of the viscous force represented by the product of the viscosity and the Laplacian of the velocity on the right-hand side.

The Eulerian form of the Navier–Stokes equation involving time and space derivatives is

$$\rho \left( \frac{\partial \mathbf{u}}{\partial t} + \mathbf{u} \cdot \nabla \mathbf{u} \right) = -\nabla p + \mu \nabla^2 \mathbf{u} + \rho \mathbf{g}. \quad (6.5.7)$$

The three Cartesian scalar components of the Navier–Stokes equation are shown in [Table 6.5.1](#).

### 6.5.1 Pressure and viscous forces

The negative of the pressure gradient on the right-hand side of (6.5.7) represents the pressure force,  $-\nabla p$ . The Laplacian of the velocity multiplied by the viscosity on the right-hand side of (6.5.7) represents the viscous force,  $\mu \nabla^2 \mathbf{u}$ .

Working in index notation under the assumption that the fluid is incompressible and therefore the velocity field is solenoidal,  $\nabla \cdot \mathbf{u} = 0$ , we find that the Laplacian of the velocity is equal to the negative of the curl of the vorticity

$$\nabla^2 \mathbf{u} = -\nabla \times \boldsymbol{\omega} \quad (6.5.8)$$

(Problem 6.5.1). An important consequence of this identity is that, if the flow is irrotational, or the vorticity is uniform, or the vorticity field is irrotational, the viscous force vanishes identically even though the fluid is not inviscid. In that case, the Navier–Stokes equation reduces to Euler’s equation, which can be integrated to yield Bernoulli’s equation (6.4.12) for irrotational flow or equation (6.4.48) for steady rotational flow.

### 6.5.2 A radially expanding or contracting bubble

An example of an irrotational flow with nonzero viscous stresses but vanishing viscous forces is provided by the flow generated by the radial expansion or contraction of a spherical bubble

with time-dependent radius,  $a(t)$ . The induced velocity field can be represented by a three-dimensional point source with time dependent strength,  $m(t)$ , placed at the center of the bubble. In spherical polar coordinates with the origin at the bubble center, the velocity potential is given by

$$\phi(r, t) = -m(t) \frac{1}{4\pi} \frac{1}{r}, \quad (6.5.9)$$

and the radial component of the velocity is given by

$$u_r(r, t) = \frac{\partial \phi}{\partial r} = m(t) \frac{1}{4\pi} \frac{1}{r^2}, \quad (6.5.10)$$

where  $r$  is the distance from the bubble center.

The no-penetration condition at the surface of the bubble requires that

$$\frac{da}{dt} = u_r(r = a), \quad (6.5.11)$$

which can be rearranged into an expression for the strength of the point source in terms of the bubble radius,

$$m(t) = 4\pi a^2(t) \frac{da}{dt}. \quad (6.5.12)$$

Substituting expression (6.5.12) into equations (6.5.9) and (6.5.10), we obtain

$$\phi(r) = -a^2(t) \frac{da}{dt} \frac{1}{r} = -\frac{1}{3} \frac{da^3}{dt} \frac{1}{r} \quad (6.5.13)$$

and

$$u_r(r) = \frac{\partial \phi}{\partial r} = \frac{1}{3} \frac{da^3}{dt} \frac{1}{r^2}. \quad (6.5.14)$$

Now referring to Bernoulli's equation (6.4.12) for unsteady irrotational flow,

$$\frac{\partial \phi}{\partial t} + \frac{1}{2} u^2 + \frac{p}{\rho} - \mathbf{g} \cdot \mathbf{x} = c(t), \quad (6.5.15)$$

we compute the first and second terms on the left-hand side,

$$\frac{\partial \phi}{\partial t} = -\frac{1}{3} \frac{d^2 a^3}{dt^2} \frac{1}{r}, \quad u^2 = u_r^2(r) = \frac{1}{9} \left( \frac{da^3}{dt} \right)^2 \frac{1}{r^4}. \quad (6.5.16)$$

Substituting these expressions into Bernoulli's equation and solving for the pressure, we derive the expression

$$\frac{p(r)}{\rho} = \frac{1}{3} \frac{d^2 a^3}{dt^2} \frac{1}{r} - \frac{1}{18} \left( \frac{da^3}{dt} \right)^2 \frac{1}{r^4} + c(t) + \mathbf{g} \cdot \mathbf{x}. \quad (6.5.17)$$

Far from the bubble, the first and second terms on the right-hand side vanish and the pressure assumes a linear and possibly time-dependent distribution,

$$p_\infty(\mathbf{x}, t) = \rho (c(t) + \mathbf{g} \cdot \mathbf{x}). \quad (6.5.18)$$

The normal stress,  $\sigma_{rr}$ , undergoes a jump across the bubble surface, determined by the mean curvature and the surface tension,  $\gamma$ . Using the simplified version of the interfacial condition (4.4.4) for an interface with uniform surface tension, we obtain

$$\sigma_{rr}(r = a) + p_B(t) = \gamma 2\kappa_m = \gamma \frac{2}{a}, \quad (6.5.19)$$

where  $p_B(t)$  is the pressure in the bubble interior and  $\kappa_m = 1/a$  is the mean curvature of the spherical interface. Substituting the second equation in (6.5.14) into the Newtonian constitutive equation

$$\sigma_{rr} = -p + 2\mu \frac{\partial u_r}{\partial r}, \quad (6.5.20)$$

and the resulting expression into (6.5.19), we find that

$$p(r = a) = p_B(t) - 4\mu \frac{da}{dt} \frac{1}{a} - \gamma \frac{2}{a}. \quad (6.5.21)$$

In the last step, we apply expression (6.5.17) at the bubble surface, evaluate the surface pressure from (6.5.21), neglect hydrostatic variations over the diameter of the bubble, and rearrange the resulting expression to obtain the generalized Rayleigh equation

$$\rho a \frac{d^2 a}{dt^2} + \frac{3}{2} \rho \left( \frac{da}{dt} \right)^2 + 4\mu \frac{da}{dt} \frac{1}{a} + \gamma \frac{2}{a} = p_B(t) - p_\infty(\mathbf{x}_B, t), \quad (6.5.22)$$

where  $\mathbf{x}_B$  is the location of the bubble center.

The evolution of the bubble radius from a given initial state is governed by the second-order nonlinear ordinary differential equation (6.5.22). To compute the solution, we require the initial bubble radius,  $a$ , the initial rate of expansion,  $da/dt$ , the bubble pressure,  $p_B$ , and the ambient liquid pressure at infinity,  $p_\infty$ . The bubble pressure may be further related to the bubble volume by an appropriate equation of state provided by thermodynamics.

### 6.5.3 Boundary conditions

The Navier–Stokes equation is a second-order differential equation for the velocity with respect to spatial coordinates. To compute a solution, we require one scalar boundary condition for each component of the velocity or traction over each boundary of the flow.

#### *Impermeable solid surface*

Over an impermeable solid surface, we require the no-penetration boundary condition and the no-slip or slip boundary condition, as discussed in Sections 2.10 and 4.8.

### Free surface

Over a free surface with uniform surface tension, we require that the tangential component of the traction vanishes, while the normal component is equal to the negative of the ambient pressure increased or decreased by the capillary pressure defined as the product of the surface tension and twice the local mean curvature, as discussed in Section 4.3.

### Fluid interface

Over a fluid interface, we require kinematic and dynamic continuity or jump conditions. The kinematic condition requires that all velocity components are continuous across the interface. The dynamic condition requires that the normal component of the traction undergoes a discontinuity by an amount that is equal to the capillary pressure, while the tangential component of the traction undergoes a discontinuity that is determined by the Marangoni traction due to variations in surface tension, as discussed in Section 4.3.

#### 6.5.4 Polar coordinates

The cylindrical polar components of the hydrodynamic volume force for a Newtonian fluid arise by substituting the constitutive relations shown in Table 4.7.1 into the expressions shown in Table 4.3.1(a). After a fair amount of algebra, we derive the expressions shown in Table 6.5.2(a). The cylindrical polar components of the Navier–Stokes equation arise by substituting these relations into the right-hand sides of (6.3.18).

The spherical polar components of the hydrodynamic volume force arise by substituting the constitutive relations given in Table 4.7.2 into the expressions shown in Table 4.3.1(b). After a fair amount of algebra, we derive the expressions shown in Table 6.5.2(b). The Laplacian operator  $\nabla^2$  in spherical polar coordinates is defined as

$$\nabla^2\phi \equiv \frac{1}{r^2} \frac{\partial}{\partial r} \left( r^2 \frac{\partial\phi}{\partial r} \right) + \frac{1}{r^2 \sin\theta} \frac{\partial}{\partial\theta} \left( \sin\theta \frac{\partial\phi}{\partial\theta} \right) + \frac{1}{r^2 \sin^2\theta} \frac{\partial^2\phi}{\partial\varphi^2} = 0. \quad (6.5.23)$$

The spherical polar components of the Navier–Stokes equation arise by substituting these expressions into the right-hand sides of (6.3.21).

The plane polar components of the hydrodynamic volume force arise by substituting the constitutive relations shown in Table 4.7.3 into the expressions shown in Table 4.3.1(c). After a fair amount of algebra, we derive the expressions shown in Table 6.5.2(c). The plane polar components of the Navier–Stokes equation arise by substituting these expressions into the right-hand sides of (6.3.24).

## PROBLEMS

### 6.5.1 Viscous force

Prove identity (6.5.8) for an incompressible fluid. *Hint:* Set the vorticity equal to the curl of the velocity, express the curl of the vorticity in index notation, and then use identity (2.3.11).

(a)

$$\begin{aligned}\Sigma_x &= -\frac{\partial p}{\partial x} + \mu \left( \frac{\partial^2 u_x}{\partial x^2} + \frac{1}{\sigma} \frac{\partial}{\partial \sigma} \left( \sigma \frac{\partial u_x}{\partial \sigma} \right) + \frac{1}{\sigma^2} \frac{\partial^2 u_x}{\partial \varphi^2} \right) \\ \Sigma_\sigma &= -\frac{\partial p}{\partial \sigma} + \mu \left( \frac{\partial^2 u_\sigma}{\partial x^2} + \frac{\partial}{\partial \sigma} \left( \frac{1}{\sigma} \frac{\partial(\sigma u_\sigma)}{\partial \sigma} \right) + \frac{1}{\sigma^2} \frac{\partial^2 u_\sigma}{\partial \varphi^2} - \frac{2}{\sigma^2} \frac{\partial u_\varphi}{\partial \varphi} \right) \\ \Sigma_\varphi &= -\frac{1}{\sigma} \frac{\partial p}{\partial \varphi} + \mu \left( \frac{\partial^2 u_\varphi}{\partial x^2} + \frac{\partial}{\partial \sigma} \left( \frac{1}{\sigma} \frac{\partial(\sigma u_\varphi)}{\partial \sigma} \right) + \frac{1}{\sigma^2} \frac{\partial^2 u_\varphi}{\partial \varphi^2} + \frac{2}{\sigma^2} \frac{\partial u_\sigma}{\partial \varphi} \right)\end{aligned}$$

(b)

$$\begin{aligned}\Sigma_r &= -\frac{\partial p}{\partial r} + \mu \left( \nabla^2 u_r - \frac{2}{r^2} u_r - \frac{2}{r^2} \frac{\partial u_\theta}{\partial \theta} - \frac{2}{r^2} u_\theta \cot \theta - \frac{2}{r^2 \sin \theta} \frac{\partial u_\varphi}{\partial \varphi} \right) \\ \Sigma_\theta &= -\frac{1}{r} \frac{\partial p}{\partial \theta} + \mu \left( \nabla^2 u_\theta + \frac{2}{r^2} \frac{\partial u_r}{\partial \theta} - \frac{u_\theta}{r^2 \sin^2 \theta} - \frac{2 \cos \theta}{r^2 \sin^2 \theta} \frac{\partial u_\varphi}{\partial \varphi} \right) \\ \Sigma_\varphi &= -\frac{1}{r \sin \theta} \frac{\partial p}{\partial \varphi} + \mu \left( \nabla^2 u_\varphi - \frac{u_\varphi}{r^2 \sin^2 \theta} + \frac{2}{r^2 \sin \theta} \frac{\partial u_r}{\partial \varphi} + \frac{2 \cos \theta}{r^2 \sin^2 \theta} \frac{\partial u_\theta}{\partial \varphi} \right)\end{aligned}$$

(c)

$$\begin{aligned}\Sigma_r &= -\frac{\partial p}{\partial r} + \mu \left( \frac{\partial}{\partial r} \left( \frac{1}{r} \frac{\partial(r u_r)}{\partial r} \right) + \frac{1}{r^2} \frac{\partial^2 u_r}{\partial \theta^2} - \frac{2}{r^2} \frac{\partial u_\theta}{\partial \varphi} \right) \\ \Sigma_\theta &= -\frac{1}{r} \frac{\partial p}{\partial \theta} + \mu \left( \frac{\partial}{\partial r} \left( \frac{1}{r} \frac{\partial(r u_\theta)}{\partial r} \right) + \frac{1}{r^2} \frac{\partial^2 u_\theta}{\partial \theta^2} + \frac{2}{r^2} \frac{\partial u_r}{\partial \theta} \right)\end{aligned}$$

**Table 6.5.2** Components of the hydrodynamic volume force for a Newtonian fluid in (a) cylindrical, (b) spherical, and (c) plane polar coordinates. The Laplacian operator  $\nabla^2$  in spherical polar coordinates is defined in equation (6.5.23).

### 6.5.2 Steady flow

Consider a flow at steady state. Explain why it is not generally possible to specify an arbitrary solenoidal velocity field that satisfies the boundary conditions, and then compute the pressure by solving the Navier–Stokes equation (6.5.7).

*Hint:* Consider the conditions for the equation  $\nabla p = \mathbf{F}$  to have a solution for  $p$ , where  $\mathbf{F}$  is a given vector field. Recall that the curl of the gradient of a scalar function vanishes, as shown in equation (6.6.20).

### 6.5.3 Expansion of a bubble

Show that, when the right-hand side of (6.5.22) vanishes and viscous stresses and surface

tension are both insignificant, an exact solution of equation (6.5.22) is

$$\frac{a(t)}{a(t=0)} = \left( 1 + \frac{5}{2} \frac{t}{a(t=0)} \left( \frac{da}{dt} \right)_{t=0} \right)^{2/5}. \quad (6.5.24)$$

Note that both the initial bubble radius and the initial rate of expansion or contraction must be specified.

## 6.6 Vorticity transport

In Section 6.3, we interpreted the equation of motion as an evolution equation determining the rate of change of the velocity (acceleration) of a point particle or the rate of change of the fluid velocity at a given point in a flow. Descendant evolution equations governing the rate of change of the spatial derivatives of the velocity comprising the velocity-gradient tensor and its symmetric and skew-symmetric components comprising the rate-of-deformation and vorticity tensors can be derived by straightforward differentiation.

Of particular interest is the evolution of the skew-symmetric part of the velocity-gradient tensor,  $\Xi$ , which is related to the vorticity,  $\boldsymbol{\omega}$ , as shown in (2.3.17),

$$\Xi_{ij} = \frac{1}{2} \epsilon_{ijk} \omega_k, \quad (6.6.1)$$

where  $\epsilon_{ijk}$  is the alternating tensor. The availability of an evolution equation for the vorticity allows us to study the rate of change of the angular velocity of small fluid parcels as they translate and deform while they are convected in a flow.

### 6.6.1 Two-dimensional flow

We begin by considering the evolution of the  $z$  vorticity component in a two-dimensional flow in the  $xy$  plane, defined in terms of the velocity as

$$\omega_z = \frac{\partial u_y}{\partial x} - \frac{\partial u_x}{\partial y}. \quad (6.6.2)$$

To derive an evolution equation for  $\omega_z$ , we divide both sides of the equation of motion (6.3.15) by the density,  $\rho$ , so as to remove it from the left-hand side, obtaining

$$\frac{\partial \mathbf{u}}{\partial t} + \mathbf{u} \cdot \nabla \mathbf{u} = \frac{1}{\rho} \boldsymbol{\Sigma} + \mathbf{g}, \quad (6.6.3)$$

where  $\boldsymbol{\Sigma} \equiv \nabla \cdot \boldsymbol{\sigma}$  is the hydrodynamic volume force. Taking the  $y$  derivative of the  $x$  component of this equation, and then subtracting the result from the  $x$  derivative of the corresponding  $y$  component, we derive the vorticity transport equation

$$\frac{\partial \omega_z}{\partial t} + \frac{\partial}{\partial x} \left( u_x \frac{\partial u_y}{\partial x} + u_y \frac{\partial u_y}{\partial y} \right) - \frac{\partial}{\partial y} \left( u_x \frac{\partial u_x}{\partial x} + u_y \frac{\partial u_x}{\partial y} \right) = \frac{\partial}{\partial x} \left( \frac{1}{\rho} \Sigma_y \right) - \frac{\partial}{\partial y} \left( \frac{1}{\rho} \Sigma_x \right). \quad (6.6.4)$$



Expanding the derivatives on the left-hand side and using the continuity equation for an incompressible fluid,

$$\frac{\partial u_x}{\partial x} + \frac{\partial u_y}{\partial y} = 0, \quad (6.6.5)$$

we obtain the simpler form

$$\frac{D\omega_z}{Dt} \equiv \frac{\partial\omega_z}{\partial t} + u_x \frac{\partial\omega_z}{\partial x} + u_y \frac{\partial\omega_z}{\partial y} = \frac{\partial}{\partial x} \left( \frac{1}{\rho} \Sigma_y \right) - \frac{\partial}{\partial y} \left( \frac{1}{\rho} \Sigma_x \right), \quad (6.6.6)$$

where  $D/Dt$  is the material derivative. The left-hand side of (6.6.6) expresses the material derivative of the vorticity, which is equal to twice the rate of change of the angular velocity of a small fluid parcel according to equation (2.3.9).

Next, we expand the derivatives on the right-hand side of (6.6.6) setting, for example,

$$\frac{\partial}{\partial x} \left( \frac{1}{\rho} \Sigma_y \right) = \frac{1}{\rho} \frac{\partial \Sigma_y}{\partial x} - \Sigma_y \frac{1}{\rho^2} \frac{\partial \rho}{\partial x}, \quad (6.6.7)$$

and express the hydrodynamic volume force in terms of the stresses using the definitions

$$\Sigma_x \equiv \frac{\partial \sigma_{xx}}{\partial x} + \frac{\partial \sigma_{yx}}{\partial y}, \quad \Sigma_y \equiv \frac{\partial \sigma_{xy}}{\partial x} + \frac{\partial \sigma_{yy}}{\partial y}. \quad (6.6.8)$$

The result is a general form of the vorticity transport equation for an incompressible fluid,

$$\frac{D\omega_z}{Dt} = \frac{1}{\rho^2} \left( -\Sigma_y \frac{\partial \rho}{\partial x} + \Sigma_x \frac{\partial \rho}{\partial y} \right) + \frac{1}{\rho} \left( \frac{\partial^2 \sigma_{xy}}{\partial x^2} - \frac{\partial^2 \sigma_{xy}}{\partial y^2} + \frac{\partial^2 (\sigma_{yy} - \sigma_{xx})}{\partial x \partial y} \right). \quad (6.6.9)$$

We recall that the density is allowed to vary with position inside an incompressible fluid.

### *Baroclinic production of vorticity*

The first term on the right-hand side of (6.6.9),

$$\frac{1}{\rho^2} \left( -\Sigma_y \frac{\partial \rho}{\partial x} + \Sigma_x \frac{\partial \rho}{\partial y} \right), \quad (6.6.10)$$

expresses production of vorticity due to density inhomogeneity, known as *baroclinic production*.

To illustrate the physical mechanism underlying this term, we consider a vertical column of fluid whose density increases upward in the direction of the  $y$  axis, so that  $\partial\rho/\partial y > 0$ , as shown in [Figure 6.6.1](#). The  $x$  component of the hydrodynamic volume force,  $\Sigma_x$ , causes the column to accelerate forward in the positive direction of the  $x$  axis. Because the density and thus the inertia of the fluid increases with elevation, the top portion accelerates less than the bottom portion. As a result, the column buckles backward, exhibiting counterclockwise rotation expressed by the second term inside the parentheses on the right-hand side of (6.6.10).

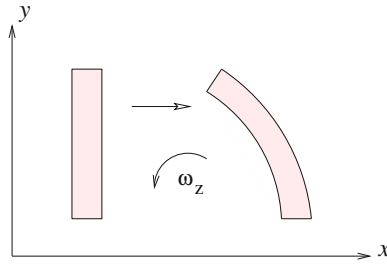


**Figure 6.6.1** Vorticity is generated when a column of fluid that is heavy at the top buckles in acceleration under the influence of a horizontal volume force.

A similar interpretation is possible in the case of a horizontal layer whose density increases in the direction of the  $x$  axis, so that  $\partial\rho/\partial x > 0$ . The preceding arguments suggest that the layer rotates under the influence of a vertical volume force,  $\Sigma_y$ . The associated baroclinic production of vorticity is expressed the first term inside the parentheses on the right-hand side of (6.6.10).

#### *Flow with negligible viscous forces*

When viscous forces are insignificant, the shear stresses virtually vanish while the normal stresses,  $\sigma_{xx}$  and  $\sigma_{yy}$ , are equal to the negative of the pressure,  $-p$ . Consequently, the term enclosed by the tall parentheses on the right-hand side of (6.6.9) makes a negligible contribution to the vorticity transport equation.

In the absence of viscous stresses, the hydrodynamic volume force is equal to the negative of the pressure gradient,  $\Sigma = -\nabla p$ . Substituting  $\Sigma_x = -\partial p/\partial x$  and  $\Sigma_y = -\partial p/\partial y$ , we find that the term expressing baroclinic production of vorticity takes a simple form, yielding the vorticity transport equation

$$\rho^2 \frac{D\omega_z}{Dt} = \frac{\partial p}{\partial y} \frac{\partial \rho}{\partial x} - \frac{\partial p}{\partial x} \frac{\partial \rho}{\partial y}. \quad (6.6.11)$$

The right-hand side can be expressed in terms of a triple mixed vector product, yielding

$$\rho^2 \frac{D\omega_z}{Dt} = (\nabla \rho \times \nabla p) \cdot \mathbf{e}_z, \quad (6.6.12)$$

where  $\mathbf{e}_z$  is the unit vector along the  $z$  axis that is perpendicular to the  $xy$  plane of the flow.

In the case of a fluid with uniform density,  $\nabla \rho = \mathbf{0}$ , equation (6.6.11) predicts that

$$\frac{D\omega_z}{Dt} = 0, \quad (6.6.13)$$

which shows that a small fluid parcel rotates with constant angular velocity as it moves about the domain of flow. The physical origin of this remarkably simple result can be traced back to conservation of angular momentum in the absence of a shearing stress imparting a torque.

Temperature °C	Water cm <sup>2</sup> /sec	Air cm <sup>2</sup> sec
20	$1.004 \times 10^{-2}$	$15.05 \times 10^{-2}$
40	$0.658 \times 10^{-2}$	$18.86 \times 10^{-2}$
80	$0.365 \times 10^{-2}$	$20.88 \times 10^{-2}$

**Table 6.6.1** The kinematic viscosity of water and air at three temperatures. Note that the kinematic viscosity of air is higher than that of water due to its much lower density.

### Incompressible Newtonian fluids

Next, we consider the evolution of vorticity in an incompressible Newtonian fluid with uniform density and viscosity. Substituting the constitutive equation for the stress tensor shown in Table 4.5.1 into the right-hand side of (6.6.9), and simplifying the resulting expression using the continuity equation, we derive the vorticity transport equation

$$\frac{\partial \omega_z}{\partial t} + u_x \frac{\partial \omega_z}{\partial x} + u_y \frac{\partial \omega_z}{\partial y} = \nu \left( \frac{\partial^2 \omega_z}{\partial x^2} + \frac{\partial^2 \omega_z}{\partial y^2} \right), \quad (6.6.14)$$

where  $\nu \equiv \mu/\rho$  is a physical constant with dimensions of length squared divided by time, called the *kinematic viscosity* of the fluid. In compact notation, the vorticity transport equation reads

$$\frac{D\omega_z}{Dt} \equiv \nu \nabla^2 \omega_z, \quad (6.6.15)$$

where  $D/Dt$  is the material derivative and  $\nabla^2$  is the Laplacian operator in the  $xy$  plane.

The kinematic viscosity of water and air is shown in Table 6.6.1 at three temperatures. Note that the kinematic viscosity of air is higher than that of water by two or three orders of magnitude. In contrast, the viscosity of water is higher than that of air by one or two orders of magnitude. Curiously, air is kinematically more viscous than water due to its lower density.

The right-hand side of (6.6.14) expresses diffusion of vorticity in the  $xy$  plane. Like temperature or concentration of a species, vorticity spreads from regions of highly rotational flow to regions of irrotational flow; that is, from regions where small spherical parcels exhibit intense rotation to regions of weakly rotational or irrotational motion. The actual mechanism by which this occurs will be exemplified in Chapters 7 and 10 with reference to unsteady and boundary-layer flow.

### 6.6.2 Axisymmetric flow

Consider an axisymmetric flow in the absence swirling motion and refer to cylindrical polar coordinates,  $(x, \sigma, \varphi)$ , as shown in Figure 6.6.2. Working as previously for two-dimensional

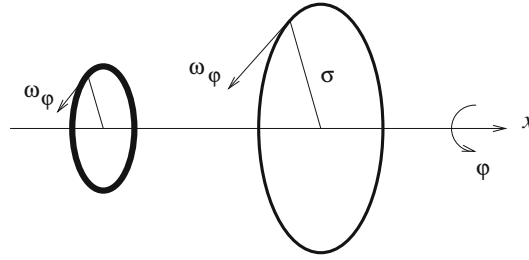


**Figure 6.6.2** The vorticity of a point particle in an axisymmetric flow increases as the particle moves farther away from the axis of symmetry due to vortex stretching.

flow, we derive the vorticity transport equation for an incompressible Newtonian fluid with uniform density and viscosity,

$$\frac{D}{Dt} \left( \frac{\omega_\varphi}{\sigma} \right) = \nu \frac{1}{\sigma^2} \mathcal{E}^2(\sigma \omega_\varphi), \quad (6.6.16)$$

where  $\sigma$  is the distance from the  $x$  axis, The second-order linear differential operator  $\mathcal{E}^2$  on the right-hand side, defined in equations (2.9.24) and (2.9.27), is the counterpart of the Laplacian operator for two-dimensional flow shown in (6.6.14).

### Vortex stretching

When viscous forces are negligible, the right-hand side of (6.6.16) is zero and the resulting vorticity transport equation takes the simple form

$$\frac{D}{Dt} \left( \frac{\omega_\varphi}{\sigma} \right) = 0. \quad (6.6.17)$$

This equation requires that the azimuthal component of the vorticity of a point particle,  $\omega_\varphi$ , is proportional to the distance of the point particle from the axis of symmetry,  $\sigma$ , so that the ratio between the two is constant in time and equal to the initial value, as illustrated schematically in Figure 6.6.2. This fundamental evolution law expresses a physical process known as *vortex stretching*. The significance of vortex stretching will be discussed in Chapter 11 in the context of vortex flow.

### 6.6.3 Three-dimensional flow

Generalizing the preceding discussion, we proceed to derive an evolution equation for the vorticity vector field in a three-dimensional incompressible Newtonian flow. The density and viscosity are assumed to be uniform throughout the domain of flow.

Our point of departure is the Navier–Stokes equation (6.4.3). Using the expression for the point particle acceleration shown on the left-hand side of equation (6.3.26), we derive the following alternative form of the Navier–Stokes equation in terms of the vortex force,

$$\rho \left( \frac{\partial \mathbf{u}}{\partial t} + \frac{1}{2} \nabla u^2 + \boldsymbol{\omega} \times \mathbf{u} \right) = -\nabla p + \mu \nabla^2 \mathbf{u} + \rho \mathbf{g}, \quad (6.6.18)$$

where

$$u^2 \equiv u_x^2 + u_y^2 + u_z^2 \quad (6.6.19)$$

is the square of the magnitude of the velocity.

To derive an evolution equation for the vorticity, we take the curl of both sides of equation (6.6.18). A vector identity states that the curl of the gradient of a smooth scalar function of position,  $f(\mathbf{x})$ , is identically zero,

$$\nabla \times \nabla f = \mathbf{0}. \quad (6.6.20)$$

To prove this identity, we work in index notation and express the  $i$ th component of the left-hand side as

$$\epsilon_{ijk} \frac{\partial}{\partial x_j} \left( \frac{\partial f}{\partial x_k} \right) = \epsilon_{ijk} \frac{\partial^2 f}{\partial x_j \partial x_k} = -\epsilon_{ikj} \frac{\partial^2 f}{\partial x_k \partial x_j}. \quad (6.6.21)$$

The symmetry of the second derivative on the right-hand side, combined with the inherent antisymmetry of the alternating tensor, ensures that the right-hand side is identically zero.

Using identity (6.6.20), we find that the curl of the second term on the left-hand side of (6.6.18), involving the square of the velocity, and the curl of the first term on the right-hand side of (6.6.18), involving the pressure gradient, are both zero. Invoking the definition of the vorticity,  $\boldsymbol{\omega} = \nabla \times \mathbf{u}$ , we obtain the vorticity transport equation for three-dimensional flow,

$$\frac{\partial \boldsymbol{\omega}}{\partial t} + \nabla \times (\boldsymbol{\omega} \times \mathbf{u}) = \nu \nabla^2 \boldsymbol{\omega}, \quad (6.6.22)$$

where  $\nu \equiv \mu/\rho$  is the kinematic viscosity of the fluid.

### *Evolution of the point particle vorticity*

The second term on the left-hand side of (6.6.22), denoted by

$$\mathcal{A} \equiv \nabla \times (\boldsymbol{\omega} \times \mathbf{u}), \quad (6.6.23)$$

can be manipulated to acquire a precise physical interpretation. In index notation,

$$\mathcal{A}_i = \epsilon_{ijk} \frac{\partial}{\partial x_j} (\epsilon_{klm} \omega_l u_m) = \epsilon_{ijk} \epsilon_{klm} \frac{\partial (\omega_l u_m)}{\partial x_j}. \quad (6.6.24)$$

Rearranging the indices, we obtain

$$\mathcal{A}_i = \epsilon_{ijk} \epsilon_{lmk} \frac{\partial (\omega_l u_m)}{\partial x_j}. \quad (6.6.25)$$

Using the property of the alternating tensor

$$\epsilon_{ijk} \epsilon_{lmk} = \delta_{il} \delta_{jm} - \delta_{im} \delta_{jl}, \quad (6.6.26)$$

we find that

$$\mathcal{A}_i = (\delta_{il} \delta_{jlm} - \delta_{im} \delta_{jl}) \frac{\partial(\omega_l u_m)}{\partial x_j} = \frac{\partial(\omega_i u_j)}{\partial x_j} - \frac{\partial(\omega_j u_i)}{\partial x_j}. \quad (6.6.27)$$

Expanding the product of the derivative on the right-hand side, we obtain

$$\mathcal{A}_i = u_j \frac{\partial \omega_i}{\partial x_j} + \omega_i \frac{\partial u_j}{\partial x_j} - u_i \frac{\partial \omega_j}{\partial x_j} - \omega_j \frac{\partial u_i}{\partial x_j}. \quad (6.6.28)$$

An identity states that the divergence of the curl of a smooth vector field is zero. A consequence of this identity is that the vorticity field is solenoidal,

$$\nabla \cdot \boldsymbol{\omega} = \nabla \cdot (\nabla \times \mathbf{u}) = 0. \quad (6.6.29)$$

Because the fluid has been assumed incompressible, the velocity field is also solenoidal,  $\nabla \cdot \mathbf{u} = 0$ . Consequently, the second and third terms on the right-hand side of (6.6.28) are zero, yielding

$$\mathcal{A}_i = u_j \frac{\partial \omega_i}{\partial x_j} - \omega_j \frac{\partial u_i}{\partial x_j}. \quad (6.6.30)$$

Substituting the result back into equation (6.6.22), we derive the targeted vorticity transport equation

$$\frac{D \omega_i}{Dt} = \frac{\partial \omega_i}{\partial t} + u_j \frac{\partial \omega_i}{\partial x_j} = \omega_j \frac{\partial u_i}{\partial x_j} + \nu \nabla^2 \omega_i. \quad (6.6.31)$$

In vector notation,

$$\frac{D \boldsymbol{\omega}}{Dt} = \frac{\partial \boldsymbol{\omega}}{\partial t} + \mathbf{u} \cdot \nabla \boldsymbol{\omega} = \boldsymbol{\omega} \cdot \nabla \mathbf{u} + \nu \nabla^2 \boldsymbol{\omega}, \quad (6.6.32)$$

where  $D\boldsymbol{\omega}/Dt$  is the material derivative of the vorticity expressing the rate of change of the vorticity vector following the motion of a point particle.

### *Vorticity rotation and vortex stretching*

To understand the nature of the first term on the right-hand side of (6.6.32),  $\boldsymbol{\omega} \cdot \nabla \mathbf{u}$ , we consider a small material vector,  $d\mathbf{X}$ , and label the first point A and the last point B. Using a Taylor series expansion, we find that the difference in the velocity across the end points is

$$\mathbf{u}^B - \mathbf{u}^A \simeq d\mathbf{X} \cdot \nabla \mathbf{u}. \quad (6.6.33)$$

Comparing this expression with the expression of interest  $\boldsymbol{\omega} \cdot \nabla \mathbf{u}$ , we find that the vorticity vector behaves like a material vector convected by the flow. This means that the vorticity vector rotates and stretches or compresses under the influence of the local flow.

In the case of two-dimensional flow, because the vorticity vector is normal to the plane of the flow, neither rotation, nor stretching, nor compression can take place. In the case of axisymmetric flow, because the vorticity vector points in direction of the azimuthal angle,  $\varphi$ , rotation is prohibited but stretching or compression can take place, as discussed in Section 6.6.2.

### *Persistence of irrotational motion in an inviscid flow*

One important consequence of the vorticity transport equation (6.6.32) is that, if the vorticity of a point particle is zero at the initial instant, it will remain zero at any time. Thus, volumes of rotational fluid remain rotational, volumes of irrotational fluid remain irrotational, and the interface between rotational and irrotational fluid remains sharp and well-defined at any time.

### *Source of vorticity in viscous flow*

In practice, because a fluid flow is always established from the state of rest, the initial vorticity distribution is zero. Since the right-hand side of the vorticity transport equation (6.6.32) vanishes throughout the fluid, the initial rate of production of vorticity is also zero, and this may suggest deceptively that the flow will remain irrotational at any time. In fact, vorticity, like heat, enters the fluid by diffusion across the boundaries. The precise mechanism by which this occurs is discussed in Chapters 7 and 10.

## PROBLEMS

### 6.6.1 *Reduction to two-dimensional flow*

Show that the vorticity transport equation (6.6.32) reproduces the transport equation (6.6.14) for the strength of the vorticity,  $\omega_z$ , in a two-dimensional flow in the  $xy$  plane.

### 6.6.2 *Convection of vorticity*

Prove the identity

$$\omega_j \frac{\partial u_i}{\partial x_j} = \omega_j \frac{\partial u_j}{\partial x_i}. \quad (6.6.34)$$

This identity allows us to express the first term on the left-hand side of (6.6.32) in the alternative form

$$\boldsymbol{\omega} \cdot \nabla \mathbf{u} = \nabla \mathbf{u} \cdot \boldsymbol{\omega}. \quad (6.6.35)$$

*Hint:* Begin with the identity  $\boldsymbol{\omega} \times \boldsymbol{\omega} = \boldsymbol{\omega} \times \nabla \times \mathbf{u} = \mathbf{0}$ , and then work in index notation using identity (2.3.11).

## 6.7 Dynamic similitude and the Reynolds number

Consider a uniform (streaming) flow along the  $x$  axis with velocity  $U_1$  past a stationary body with designated size  $L_1$ , as illustrated in Figure 6.7.1(a). Also consider another streaming

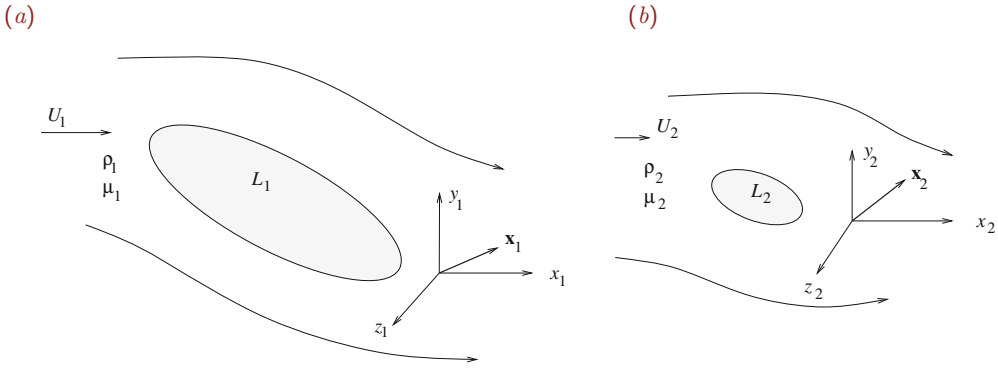


**Figure 6.7.1** Illustration of flow in two similar domains. If the Reynolds numbers of the two flows are equal, as shown in equation (6.7.10), the velocity and pressure field of the second flow may be deduced those in the first flow, and *vice versa*, by rescaling.

flow along the  $x$  axis with velocity  $U_2$  past a second body that arises by shrinking or expanding the first body by a certain factor,  $\alpha$ , as illustrated in [Figure 6.7.1\(b\)](#). If the second body is smaller than the first body,  $\alpha < 1$ ; if the second body is larger than the first body,  $\alpha > 1$ .

If the surface of the first body is described by an equation of the general form

$$f_1(x_1, y_1, z_1) = 0, \tag{6.7.1}$$

then the surface of the second body is described by the equation

$$f_2(x_2, y_2, z_2) = f_1\left(\frac{x_2}{\alpha}, \frac{y_2}{\alpha}, \frac{z_2}{\alpha}\right) = 0, \tag{6.7.2}$$

where

$$\alpha \equiv \frac{L_2}{L_1} \tag{6.7.3}$$

is a scaling factor. Corresponding points on the first and second body are related by  $\mathbf{x}_2 = \alpha \mathbf{x}_1$ .

**A sphere**

For example, if the first body is a sphere of radius  $L_1$  centered at a point,  $\mathbf{x}_{c_1} = (x_{c_1}, y_{c_1}, z_{c_1})$ , then the equation describing the surface of this body is

$$f_1(x_1, y_1, z_1) = (x_1 - x_{c_1})^2 + (y_1 - y_{c_1})^2 + (z_1 - z_{c_1})^2 - L_1^2 = 0 \tag{6.7.4}$$

and the equation describing the surface of the second body is

$$f_2(x_2, y_2, z_2) = f_1\left(\frac{x_2}{\alpha}, \frac{y_2}{\alpha}, \frac{z_2}{\alpha}\right) \tag{6.7.5}$$



or

$$f_2(x_2, y_2, z_2) = \left(\frac{x_2}{\alpha} - x_{c_1}\right)^2 + \left(\frac{y_2}{\alpha} - y_{c_1}\right)^2 + \left(\frac{z_2}{\alpha} - z_{c_1}\right)^2 - L_1^2 = 0. \quad (6.7.6)$$

Simplifying, we obtain

$$f_2(x_2, y_2, z_2) = \frac{1}{\alpha^2} \left( (x_2 - \alpha x_{c_1})^2 + (y_2 - \alpha y_{c_1})^2 + (z_2 - \alpha z_{c_1})^2 - L_2^2 \right) = 0, \quad (6.7.7)$$

which the equation of a sphere of radius  $L_2 = \alpha L_1$  centered at the point  $\mathbf{x}_{c_2} = \alpha \mathbf{x}_{c_1}$ . We may set without loss of generality  $\mathbf{x}_{c_1} = \mathbf{0}$ , in which case both spheres are centered at the origin.

### Reynolds number

Let  $\rho_1$  and  $\mu_1$  be the density and viscosity of the first fluid, and  $\rho_2$  and  $\mu_2$  be the density and viscosity of the second fluid. Both fluids are assumed to be incompressible and Newtonian. We will show that, when the values of the four control and physical parameters defining the first flow,

$$L_1, \quad U_1, \quad \rho_1, \quad \mu_1, \quad (6.7.8)$$

and the corresponding values of the four control and physical parameters defining the second flow,

$$L_2, \quad U_2, \quad \rho_2, \quad \mu_2, \quad (6.7.9)$$

are related by the equation

$$\frac{\rho_1 U_1 L_1}{\mu_1} = \frac{\rho_2 U_2 L_2}{\mu_2}, \quad (6.7.10)$$

then the structure of the second flow can be inferred from the structure of the first flow, and *vice versa*, by a simple computation described as rescaling. The left-hand side of (6.7.10) is the Reynolds number of the first flow, and the right-hand side of (6.7.10) is the Reynolds number of the second flow.

### Rescaling

To deduce the structure of the second flow from the structure of the first flow, we introduce the dynamic pressure established due to the flow, defined as the pressure deviation from the hydrostatic distribution,

$$\varsigma_1 \equiv p_1 - \rho_1 \mathbf{g} \cdot \mathbf{x}_1, \quad \varsigma_2 \equiv p_2 - \rho_2 \mathbf{g} \cdot \mathbf{x}_2. \quad (6.7.11)$$

In the absence of flow, the pressure assumes the hydrostatic distribution and the dynamic pressure vanishes throughout both domains of flow.

Now we consider an arbitrary point in the first flow,  $\mathbf{x}_1$ , and a corresponding point in the second flow whose coordinates are given by

$$\mathbf{x}_2 = \alpha \mathbf{x}_1. \quad (6.7.12)$$

Equations (6.7.1) and (6.7.2) ensure that, if the point  $\mathbf{x}_1$  lies at the surface of the body in the first flow, then the point  $\mathbf{x}_2$  will lie at the surface of the body in the second flow.

We will demonstrate that, when relation (6.7.10) is fulfilled, the velocity and dynamic pressure at the point  $\mathbf{x}_2$  in the second flow are related to those at the point  $\mathbf{x}_1$  in the first flow by the equations

$$\mathbf{u}_2(\mathbf{x}_2) = \delta \mathbf{u}_1(\mathbf{x}_1), \quad \varsigma_2(\mathbf{x}_2) = \beta \delta^2 \varsigma_1(\mathbf{x}_1), \quad (6.7.13)$$

where  $\delta$  is the ratio of the velocities of the incident flow and  $\beta$  is the density ratio,

$$\delta \equiv \frac{U_2}{U_1}, \quad \beta \equiv \frac{\rho_2}{\rho_1}. \quad (6.7.14)$$

The equality of the Reynolds numbers expressed by (6.7.10) requires that

$$\beta \delta = \alpha \lambda, \quad (6.7.15)$$

where

$$\lambda \equiv \frac{\mu_2}{\mu_1} \quad (6.7.16)$$

is the viscosity ratio.

### *Unsteady flow*

Relations (6.7.13) are also valid for unsteady flow, provided that the velocity field of the first flow at the designated origin of time is related to the velocity of the second flow at the designated origin of time by the first of equations (6.7.13), and the comparison is made at times  $t_1$  and  $t_2$  related by

$$t_2 = \frac{\delta}{\alpha} t_1. \quad (6.7.17)$$

A implicit assumption is that both flows have been started at the same time.

#### **6.7.1 Dimensional analysis**

To prove relations (6.7.13), we consider the Navier–Stokes equation (6.5.7),

$$\rho \left( \frac{\partial \mathbf{u}}{\partial t} + \mathbf{u} \cdot \nabla \mathbf{u} \right) = -\nabla p + \mu \nabla^2 \mathbf{u} + \rho \mathbf{g}, \quad (6.7.18)$$

and the continuity equation for an incompressible fluid,

$$\nabla \cdot \mathbf{u} = 0, \quad (6.7.19)$$

governing the structure and dynamics of each flow with appropriate physical constants corresponding to the two fluids, subject to appropriate far-field and boundary conditions, and work in three stages.

*First flow*

In the first stage, we consider the first flow and introduce the dimensionless independent variables

$$\hat{x}_1 = \frac{x_1}{L_1}, \quad \hat{y}_1 = \frac{y_1}{L_1}, \quad \hat{z}_1 = \frac{z_1}{L_1}, \quad \hat{t}_1 = \frac{t_1 U_1}{L_1}, \quad (6.7.20)$$

and the dimensionless dependent variables

$$\hat{u}_{x_1} = \frac{u_{x_1}}{U_1}, \quad \hat{u}_{y_1} = \frac{u_{y_1}}{U_1}, \quad \hat{u}_{z_1} = \frac{u_{z_1}}{U_1}, \quad \hat{s}_1 = \frac{s_1}{\rho_1 U_1^2}, \quad (6.7.21)$$

all indicated by a caret (hat). Solving for the dimensional variables in terms of their dimensionless counterparts, and substituting the result into the Navier–Stokes equation and the continuity equation, we obtain

$$\frac{\partial \hat{\mathbf{u}}_1}{\partial \hat{t}_1} + \hat{\mathbf{u}}_1 \cdot \hat{\nabla}_1 \hat{\mathbf{u}}_1 = -\hat{\nabla}_1 \hat{s}_1 + \frac{1}{\text{Re}_1} \hat{\nabla}_1^2 \hat{\mathbf{u}}_1 \quad (6.7.22)$$

and

$$\hat{\nabla}_1 \cdot \hat{\mathbf{u}}_1 = 0, \quad (6.7.23)$$

where

$$\text{Re}_1 \equiv \frac{\rho_1 U_1 L_1}{\mu_1} \quad (6.7.24)$$

is the Reynolds number of the first flow, as shown on the left-hand side of (6.7.10). We have introduced the dimensionless gradient and associated Laplacian operator

$$\hat{\nabla}_1 \equiv \left( \frac{\partial}{\partial \hat{x}_1}, \quad \frac{\partial}{\partial \hat{y}_1}, \quad \frac{\partial}{\partial \hat{z}_1} \right), \quad \hat{\nabla}_1^2 \equiv \frac{\partial^2}{\partial \hat{x}_1^2} + \frac{\partial^2}{\partial \hat{y}_1^2} + \frac{\partial^2}{\partial \hat{z}_1^2}. \quad (6.7.25)$$

The far-field condition requires that, far from the body, the dimensionless velocity components  $\hat{u}_{x_1}$  tends to unity, whereas  $\hat{u}_{y_1}$  and  $\hat{u}_{z_1}$  decay to zero. The no-slip and no-penetration boundary conditions require that the velocity vanishes at points  $(x_1, y_1, z_1)$  that satisfy equation (6.7.1) or, equivalently, points  $(\hat{x}_1, \hat{y}_1, \hat{z}_1)$  that satisfy the equation

$$f_1(L_1 \hat{x}_1, L_1 \hat{y}_1, L_1 \hat{z}_1) = 0 \quad (6.7.26)$$

in dimensionless space.

*Second flow*

In the second stage, we consider the second flow and introduce the dimensionless independent variables

$$\hat{x}_2 = \frac{x_2}{L_2}, \quad \hat{y}_2 = \frac{y_2}{L_2}, \quad \hat{z}_2 = \frac{z_2}{L_2}, \quad \hat{t}_2 = \frac{t_2 U_2}{L_2}, \quad (6.7.27)$$

and the dimensionless dependent variables

$$\hat{u}_{x_2} = \frac{u_{x_2}}{U_2}, \quad \hat{u}_{y_2} = \frac{u_{y_2}}{U_2}, \quad \hat{u}_{z_2} = \frac{u_{z_2}}{U_2}, \quad \hat{s}_2 = \frac{s_2}{\rho_2 U_2^2}. \quad (6.7.28)$$

Solving for the dimensional variables in terms of their dimensionless counterparts, and substituting the result into the Navier–Stokes and continuity equation, we find that

$$\frac{\partial \hat{\mathbf{u}}_2}{\partial \hat{t}_2} + \hat{\mathbf{u}}_2 \cdot \hat{\nabla}_2 \hat{\mathbf{u}}_2 = -\hat{\nabla}_2 \hat{s}_2 + \frac{1}{\text{Re}_2} \hat{\nabla}_2^2 \hat{\mathbf{u}}_2 \quad (6.7.29)$$

and

$$\hat{\nabla}_2 \cdot \hat{\mathbf{u}}_2 = 0, \quad (6.7.30)$$

where

$$\text{Re}_2 \equiv \frac{\rho_2 U_2 L_2}{\mu_2} \quad (6.7.31)$$

is the Reynolds number of the second flow, as shown on the right-hand side of (6.7.10). We have introduced the dimensionless gradient and associated Laplacian operator

$$\hat{\nabla}_2 \equiv \left( \frac{\partial}{\partial \hat{x}_2}, \quad \frac{\partial}{\partial \hat{y}_2}, \quad \frac{\partial}{\partial \hat{z}_2} \right), \quad \hat{\nabla}_2^2 \equiv \frac{\partial^2}{\partial \hat{x}_2^2} + \frac{\partial^2}{\partial \hat{y}_2^2} + \frac{\partial^2}{\partial \hat{z}_2^2}. \quad (6.7.32)$$

The far-field condition requires that the dimensionless velocity component  $\hat{u}_{x_2}$  tends to unity, whereas  $\hat{u}_{y_2}$  and  $\hat{u}_{z_2}$  decay to zero far from the body. The no-slip and no-penetration boundary conditions require that the velocity vanishes at points  $(x_2, y_2, z_2)$  that satisfy equation (6.7.2) or, equivalently, points  $(\hat{x}_2, \hat{y}_2, \hat{z}_2)$  that satisfy the equation

$$f_1(L_1 \hat{x}_2, L_1 \hat{y}_2, L_1 \hat{z}_2) = 0 \quad (6.7.33)$$

in dimensionless space.

### Comparison

In the third stage, we compare one by one corresponding equations and boundary conditions governing the two flows in the dimensionless variables indicated by a hat, and draw four important conclusions:

1. The Navier–Stokes equation (6.7.22) is identical to the Navier–Stokes equation (6.7.29), provided that the two Reynolds numbers are equal,  $\text{Re}_1 = \text{Re}_2$ , as stated in (6.7.10).
2. The continuity equation (6.7.23) is identical to the continuity equation (6.7.30) independent of the Reynolds numbers.
3. The far-field conditions are identical: both dimensionless velocities designated by a caret tend to  $[1, 0, 0]$  far from the body.

4. The boundary conditions on the first body described by (6.7.26) are identical to the boundary conditions on the second body described by (6.7.33).

These results demonstrate that, when the Reynolds numbers of the two flows are equal, values of the dimensionless dependent variables in the two flows at corresponding dimensionless times and dimensionless positions are the same. For example, setting

$$\widehat{\varsigma}_1(\widehat{\mathbf{x}}_1) = \widehat{\varsigma}_2(\widehat{\mathbf{x}}_2) \quad (6.7.34)$$

and using the definitions (6.7.21) and (6.7.28), we derive the second relation in (6.7.13), subject to the definitions given in (6.7.14).

An important implication of the scaling analysis is that a flow of interest in a large domain, such as the flow past an aircraft, can be studied conveniently in a miniaturized geometry. Conversely, a flow of interest in a small domain, such as the flow over a small pit due to surface corrosion, can be studied conveniently in an enlarged domain.

## PROBLEM

### 6.7.1 Reynolds number

Compute the Reynolds number of (a) an ant crawling, (b) a person running, (c) a car moving at 100 km per hour, and (d) an elephant running across a plain at maximum speed.

## 6.8 Structure of a flow as a function of the Reynolds number

Consider the flow of an incompressible fluid in a domain with characteristic length  $L$ , identify an appropriate characteristic velocity,  $U$ , and compute the Reynolds number

$$\text{Re} \equiv \frac{\rho LU}{\mu} = \frac{LU}{\nu}, \quad (6.8.1)$$

where  $\nu \equiv \mu/\rho$  is the kinematic viscosity of the fluid. Next, introduce the dimensionless independent variables

$$\widehat{x} = \frac{x}{L}, \quad \widehat{y} = \frac{y}{L}, \quad \widehat{z} = \frac{z}{L}, \quad \widehat{t} = \frac{tU}{L}, \quad (6.8.2)$$

and the dimensionless dependent variables

$$\widehat{u}_x = \frac{u_x}{U}, \quad \widehat{u}_y = \frac{u_y}{U}, \quad \widehat{u}_z = \frac{u_z}{U}, \quad \widehat{\varsigma} = \frac{\varsigma}{\rho U^2}, \quad (6.8.3)$$

where  $\varsigma$  is the dynamic pressure excluding variations in hydrostatics. Solving for the dimensional variables in terms of their dimensionless counterparts and substituting the result into the Navier–Stokes equation and the continuity equation, we obtain the dimensionless forms

$$\frac{\partial \widehat{\mathbf{u}}}{\partial \widehat{t}} + \widehat{\mathbf{u}} \cdot \widehat{\nabla} \widehat{\mathbf{u}} = -\widehat{\nabla} \widehat{\varsigma} + \frac{1}{\text{Re}} \widehat{\nabla}^2 \widehat{\mathbf{u}} \quad (6.8.4)$$

and

$$\widehat{\nabla} \cdot \widehat{\mathbf{u}} = 0. \quad (6.8.5)$$

These dimensionless forms reveal that, given the boundary shape, the structure of a flow is determined by  $L$ ,  $U$ ,  $\rho$ , and  $\mu$  collectively through the dimensionless Reynolds number rather than individually, in the sense of the dynamic similitude expressed by equations (6.7.13) and (6.7.14).

### Velocity and length scales

The choice of characteristic velocity,  $U$ , and length scale,  $L$ , is not always apparent. Subtleties arise when the domain of flow contains an intrinsic length scale or a multitude of length scales. Examples include the flow of a suspension of small particles and the flow established spontaneously due to a hydrodynamic instability, in the absence of external forcing.

For the successful choices of  $L$  and  $U$ , all terms in the dimensionless Navier–Stokes equation (6.8.4), with the possible exception of the pressure gradient term, are of order unity. The Reynolds number then expresses the relative importance of inertial forces, assumed to scale with  $\rho U^2/L$ , and viscous forces, assumed to scale with  $\mu U/L^2$ . Their ratio is precisely the Reynolds number defined in (6.8.1).

#### 6.8.1 Stokes flow

If the Reynolds number is small, viscous forces dominate in that the left-hand side of the dimensionless Navier–Stokes equation (6.8.4) makes a negligible contribution to the underlying balance. Although the dimensionless pressure gradient also appears to make a negligible contribution, this is only a mathematical illusion.

To see this, we observe that the dimensionless pressure arose from the arbitrary scaling shown in the equation in (6.8.3), which can be contrasted with the physical scaling of the position vector and velocity in terms of the unambiguous length and velocity scales,  $L$  and  $U$ . As a consequence, the dimensionless pressure gradient may become singular as the Reynolds number tends to zero, requiring an alternative scaling. To prevent this failure, we retain the pressure gradient in the dimensionless form of the Navier–Stokes equation irrespective of the Reynolds number.

Reverting to dimensional variables, we find that the Navier–Stokes equation reduces to the Stokes equation,

$$\mathbf{0} = -\nabla p + \mu \nabla^2 \mathbf{u} + \rho \mathbf{g}, \quad (6.8.6)$$

which describes steady or unsteady creeping flow with negligible inertial forces. cursory inspection reveals that the pressure scales with  $\mu U/L$  rather than  $\rho U^2$ . The analysis and computation of creeping flow will be the exclusive topic of Chapter 9.

### 6.8.2 Flows at high Reynolds numbers

Inspecting (6.8.4), we find that, when the Reynolds number is high, viscous forces can be neglected, provided that the velocity does not change rapidly over a small distance across a fluid layer that is thin compared to the global size of the boundaries. Otherwise, the standard scaling with respect to  $U$  and  $L$  may cease to be valid.

Thin layers supporting large velocity differences typically occur along flow boundaries or interfaces between two adjacent streams of the same fluid or different fluids. In Chapter 10, we will see that viscous forces are significant inside these layers, even though the bulk of the flow may occur at high Reynolds numbers.

### 6.8.3 Laminar and turbulent flow

When the Reynolds number exceeds a certain threshold, an unsteady small-scale motion characterized by rapid fluctuations in the velocity and vorticity fields is spontaneously established. In practice, turbulent motion is often superposed on a steady or unsteady macroscopic or large-scale flow that evolves at a slower rate. A flow below the critical Reynolds number is called *laminar* to indicate that the streamlines are smooth, whereas a flow above the critical Reynolds number is called *turbulent* to indicate that the streamlines are highly convoluted.

#### Transition to turbulence

The transition from laminar to turbulent flow may occur by several venues, including the amplification of spontaneous internal waves. The critical Reynolds number where transition occurs can be estimated theoretically by carrying out a stability analysis, as discussed in Chapter 10. The dynamics of turbulent motion can be studied by several methods, including statistical analysis, nonlinear dynamical systems theory, and vortex dynamics.

## PROBLEMS

### 6.8.1 Characteristic scales

Identify the characteristic velocity scale,  $U$ , length scale,  $L$ , and Reynolds number of (a) simple shear flow past a stationary body, (b) flow due to the settling of a small particle in the atmosphere, and (c) flow due to a breaking wave in the ocean.

## 6.9 Dimensionless numbers in fluid dynamics

We have demonstrated that two geometrically related flows occurring at the same Reynolds number are similar, in that one flow can be deduced from the other by rescaling. Arguments have been made for a flow that is bounded by a solid surface over which the no-slip and no-penetration boundary conditions apply. A time-independent velocity field was imposed in the far field as a driving mechanism.

If the driving mechanism is time dependent or the flow is bounded by fluid interfaces and free surfaces, additional conditions for dynamic similitude requiring the equality of further dimensionless numbers are necessary. These dimensionless numbers enter the problem formulation either through the governing equations or through boundary and interfacial conditions.

### *Frequency number for a time-dependent flow*

Let us consider an externally forced time-dependent flow and identify a velocity scale,  $U$ , a length scale,  $L$ , and a time scale,  $T$ . In the case of periodic flow with angular frequency  $\omega$  due, for example, to an oscillating pressure gradient,  $T$  can be identified with the period,  $T = 2\pi/\omega$ . The relative importance of inertial and viscous forces in the equation of motion is expressed by the dimensionless frequency parameter

$$\beta \equiv \frac{L^2}{\nu T}, \quad (6.9.1)$$

where  $\nu$  is the kinematic viscosity of the fluid. In the case of an intrinsically time-dependent flow,  $T = L/U$ , the frequency parameter reduces to the Reynolds number  $\beta = \text{Re} = LU/\nu$ .

### *Froude number*

Consider flow in the ocean due to the propagation of water waves. The relative importance of inertial and gravitational forces is determined by the Froude number,

$$\text{Fr} \equiv \frac{U}{\sqrt{gL}}, \quad (6.9.2)$$

where  $g$  is the magnitude of the acceleration of gravity. In the case of flow over a hump discussed in Section 6.4, the Froude number takes the specific form shown in equation (6.4.43).

### *Bond number*

The relative importance of gravitational forces and surface tension in a fluid that is confined by a free surface or fluid interface is determined by the Bond number,

$$\text{Bo} \equiv \frac{\rho g L^2}{\gamma}, \quad (6.9.3)$$

where  $\gamma$  is the surface tension (Problem 6.9.1).

### *Weber number*

The relative importance of inertial forces and surface tension in a flow that is confined by a free surface or fluid interface is determined by the Weber number,

$$\text{We} \equiv \frac{\rho U^2 L}{\gamma}. \quad (6.9.4)$$



For example, the Weber number determines the deformation and structure of the flow around a gas bubble rising or convected at high speed through an ambient liquid.

### *Capillary number*

The relative importance of viscous forces and surface tension in a fluid bounded by a free surface or fluid interface is determined by the capillary number,

$$\text{Ca} \equiv \frac{\mu U}{\gamma}. \quad (6.9.5)$$

For example, the capillary number determines the deformation and thus the structure of the flow around a liquid droplet immersed in a shear flow.

## **PROBLEMS**

### **6.9.1** *Bond number in hydrostatics*

Explain how the Bond number arises from the scaling of the Laplace-Young equation (5.4.8) in hydrostatics.

### **6.9.2** *Ratio of two numbers*

What is the ratio between the Weber number and the capillary number?